

A Generalized Natural Hazard Risk Modelling Framework for Infrastructure Failure Cascades

Evelyn Mühlhofer^{a,b*}, Elco E. Koks^c, Chahan M. Kropf^{a,b}, Giovanni Sansavini^d, David N. Bresch^{a,b}

^a *Institute for Environmental Decisions, ETH Zurich, Zurich, 8092, Switzerland*

^b *Federal Office of Meteorology and Climatology MeteoSwiss, Zurich-Airport, 8058, Switzerland*

^c *Institute for Environmental Studies, VU Amsterdam, Amsterdam, The Netherlands*

^d *Institute of Energy and Process Engineering, ETH Zurich, Zurich, 8092, Switzerland*

*corresponding author (evelyn.muelhofer@usys.ethz.ch)

pre-print submitted to EarthArXiv

original in peer-review process for publication in Reliability Engineering & Systems Safety

Abstract

1 Critical infrastructures are more exposed than ever to natural hazards in a changing climate. To understand and
2 manage risk, failure cascades across large, real-world infrastructure networks, and their impact on people, must
3 be captured. Bridging established methods in both infrastructure and risk modelling communities, we develop
4 an open-source modelling framework which integrates a network-based interdependent infrastructure system
5 model into the globally consistent and spatially explicit natural hazard risk assessment platform CLIMADA. The
6 model captures infrastructure damages, triggers failure cascades and estimates resulting basic service
7 disruptions for the dependent population. It flexibly operates on large areas with publicly available hazard,
8 exposure and vulnerability information, for any set of infrastructure networks, hazards and geographies of
9 interest. In a validated case study for 2018's Hurricane Michael across three US states, the model reproduced
10 important failure dynamics among six infrastructure networks, and provided a novel spatial map where people
11 were likely to experience disruptions in access to healthcare, loss of power and other vital services. Our
12 generalized approach allows for a view on infrastructure risks and their social impacts also in areas where
13 detailed information and risk assessments are traditionally scarce, informing humanitarian activities through
14 hotspot analyses and policy frameworks alike.

15 Highlights

16

- 17 • Seamless framework, from natural hazards to infrastructure failures and basic service disruptions
- 18 • Designed for risk assessments of large-scale, real-world interdependent infrastructure systems
- 19 • Features an open-source code base, tailored to use publicly available data across many world regions
- 20 • Validated model demonstration for a historic hurricane across 3 US states and 6 infrastructure systems

21

22 Keywords

23 Risk assessment, natural hazards, critical infrastructures, failure cascades, basic service disruptions, system-of-
24 systems

25 1. Introduction

26 When natural hazards disrupt critical infrastructures (CIs), their failure can be detrimental to public health,
27 safety, security, well-being and economic activities. Whether due to an earthquake in Japan, a flooding
28 across Western Europe or a hurricane hitting the US, lifeline disruptions are ubiquitous: loss of power and
29 telecommunication services may compound with a dysfunctional transport system and damaged hospitals,
30 preventing emergency responders to intervene timely, rendering villages inaccessible for days, cutting off
31 evacuation routes, or leaving school children without access to education for up to weeks [1]–[4].

32 As infrastructure investments are at an all-time high [5], CI systems around the globe are more than ever
33 exposed to natural hazards, a trend which is further exacerbated in a changing climate [6]. This poses a
34 threat to air, road and rail transportation alike [7], [8], puts power generation at risk [9] and causes losses
35 of billions of US dollars annually in several CI sectors [8], [9].

36 Since societal impacts of CI failures tend to reach far beyond the technical sphere, managing resilient
37 infrastructure has become a prime area of concern for policy makers: CIs “directly or indirectly influence
38 the attainment of all of the SDGs” [5] and may accrue up to 88% of all climate adaptation costs until 2050
39 [10]. Reducing CIs damages and basic service disruptions forms part of the agendas of the Sendai
40 Framework for Disaster Risk Reduction, the European Commission’s Programme for Critical Infrastructure
41 Protection (EPCIP) and the 26th UN Climate Change Conference (COP26) alike. Though different in scope
42 and nature, three key challenges of CIs in a socio-technical context are recurrent: Knowledge on the extent
43 to which CIs are exposed to natural hazards is insufficient, especially in the Global South (cf. §25 e and f in
44 [11]); interdependences between different CIs are often poorly understood, and cascading effects from CI
45 failures are difficult to analyse and hence manage systematically [12], [13]; the experienced hardship from
46 CI failures depends on the degree and duration to which basic services are disrupted [14], yet the link
47 between infrastructure damages, resulting service outages and affected population is not straightforward.
48 Capturing the response of interdependent CI systems to natural hazards, and studying the impacts of their
49 failures onto the population, is an endeavour residing at the intersection of natural hazard (NH) risk
50 modelling, infrastructure modelling and social vulnerability research. Traditionally, those problems have
51 been approached with community-specific research questions and methods:

52 NH risks emerge through the interplay of weather and climate-related hazards, the exposure of
53 (infrastructure) assets, goods and people to those hazards and their specific vulnerabilities (IPCC 2014).
54 Event-based impact modelling therefore commonly relies on those three components to calculate
55 expectable asset damages to CIs as a proxy of direct risk [15]. Efforts to capture risk levels for CIs globally
56 are often challenged by data availability (cf. [16]), yet have been undertaken for a few hazards and CI
57 sectors such as road, rail, airports and power generation [7], [8], [17]. Despite acknowledging the
58 importance to embrace a systems-thinking approach for resilience [18], [19], NH risk modelers’
59 predominant focus on ‘asset scale risk’ [19] often runs short of capturing CI interdependencies and

60 'network scale risks'. As such, the community's risk assessment methods are not yet tailored to the
61 specificities of CIs.

62 In infrastructure research, CI interdependences and failure cascades have received much attention since
63 the seminal work of Rinaldi et al. [13] and approaches to model them have converged to several state-of-
64 the-art methods, comprehensively summarized in Ouyang [20]. Especially in studies employing network
65 (flow) approaches (cf. [21]), research on failure cascades is often motivated by NH events as triggers [22]–
66 [27]. Yet, most research in this domain shares some of the following tendencies: Investigated systems are
67 mostly small-scale, representative of mid-sized towns or single community districts and illustrate dynamics
68 for a sub-system of two infrastructure types [26], [28]–[31] (see [23], [25], [32] for counter-examples)
69 where power, transport and telecommunication systems are investigated much more often than social
70 facilities such as schools or hospitals. CI data is frequently based on artificial, well-defined test-beds [22],
71 [31], [33], [34], or tailored to the (sometimes proprietary) data at hand, which is overwhelmingly based in
72 the US, Europe and Oceania [23], [30], [35], [36]. Failure scenarios often focus on random or component-
73 wise removals [32], [37], [38], or feature stylized shapes in lack of realistic hazard footprints [23], [33].
74 Study scopes and trigger mechanisms in existing CI research are hence not necessarily tailored to capture
75 the magnitude and spatial extents of real-world NH events and CI systems.

76 Lastly, the technical discourse on CI failures, where impact metrics focus predominantly on functional
77 performance benchmarks, does not link adequately to the domain of social vulnerabilities [39]. Apart from
78 empirical case-studies using print media accounts [40], only few modelling studies have explored
79 consequences of CI failures for (socio-economically different groups of) people [41], [42].

80 Despite advances in tackling this common problem space, silos persist which have inspired several stylized
81 and theoretical frameworks on systemic CI risks at a national analysis level [19], [43]. Following this logic,
82 our aim is to practically implement a flexible and open-source end-to-end impact model which estimates
83 spatial patterns of people experiencing basic service disruptions caused by natural hazard-induced CI
84 failure cascades. In line with Zio [44], who stresses the need to integrate different modelling perspectives
85 to capture complexities of CI system failures, we showcase how synergies can be yielded by combining
86 established methods and platforms used by CI researchers and NH risk modellers alike. The design focus of
87 this seamless impact model is put particularly on the rapid analysis of large, interdependent, real-world
88 infrastructure systems and the dependent population in diverse geographical regions, which are exposed
89 to different types of natural hazards and where only limited process knowledge and data may be available.
90 Impact estimates produced with this approach are hence thought to inform rapid hotspot assessments
91 during emergency responses, or as a cross-national, human-centric measure of risk for policy purposes in
92 international frameworks.

93 Section 2 describes the conceptual framework which was constructed to meet above-mentioned design
94 criteria and its concrete implementation as a 'system-of-systems' [43] formulation for infrastructure
95 networks embedded in the open-source risk modelling platform CLIMADA [45]. Section 3 exemplarily

96 illustrates how the model can provide information services in the aftermath of disaster using a real-world
 97 case study of Hurricane Michael hitting the Florida Panhandle. A scenario analysis is performed and model
 98 outputs are validated using official reports and print media accounts, to facilitate a wider discussion on the
 99 merits and trade-offs of this approach in section 4, and to examine its adequacy for use in risk assessments,
 100 emergency response, adaptation planning and policy making.

101 2. Methods

102 The framework in Figure 2.1 illustrates the major conceptual stages developed to calculate basic service
 103 disruptions from natural hazard-induced infrastructure failure cascades, with required inputs and main
 104 outputs.

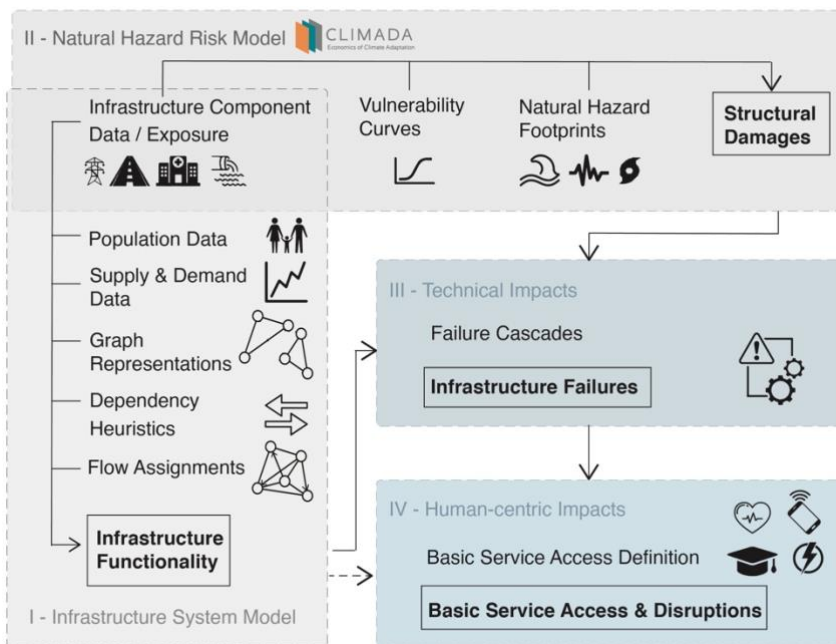


Figure 2.1 Developed framework to model the population experiencing basic service disruptions from natural hazard-induced infrastructure failure cascades. The four stages are linked within a single platform and encompass infrastructure system modelling (I), natural hazard risk modelling (II), and two spatially explicit results layers - impacts to infrastructure components (III) and to the dependent population (IV). Main outputs of each stage are in bold within a box.

105 In stage I an infrastructure system model calculates functional states of interdependent critical
 106 infrastructures using georeferenced information on infrastructure components, dependent population,
 107 dependency heuristics and supply and demand data. The employed modelling approach relies on a ‘system-
 108 of-systems’ formulation logic (cf. [23], [32], [43]), where CI systems are treated as hierarchical topological
 109 networks interconnected through dependencies between each other. The reliance on complex network
 110 theory and simpler flow calculations reduces the complexity of full-fledged physical models, yet has been
 111 demonstrated as a versatile, illustrative and data-efficient alternative capable of capturing large-scale
 112 dynamics across big system scales [23]. In stage II, structural damages to infrastructure components are
 113 computed from spatially- explicit hazard footprints and tailored vulnerability curves, using the risk
 114 assessment platform CLIMADA, which was in turn chosen for its state-of-the art performance in hazard
 115 modelling, global consistency and open-source character. Stage III feeds results from structural damage

116 calculations back into the infrastructure system model, which triggers failures cascades along infrastructure
117 dependencies. Results of this stage are technical failures at the infrastructure systems level. In stage IV,
118 technical impacts of CI failures are translated to human-centric impacts. Resulting disruptions to basic
119 service access are computed for all services provided by the CI systems under study, for the dependent
120 population.

121 The following sections describe the implementation details of the framework. While emphasis is put on
122 the conceptual choices that were made to unite models from natural hazard risk and infrastructure
123 modelling communities, specific technical explanations referring to the practical open-source code base
124 implementation are provided where necessary. For a list of abbreviations used throughout the text and a
125 condensed formal description of the entire algorithm, see annex A.

126 **2.1. Stage I: Infrastructure System Model**

127 **2.1.1. Data Requirements: Infrastructure Components, Population, Supply and Demand**

128 Geographic data of *CI networks* - henceforth referring to the spatial representation of real-world
129 infrastructures such as the location of schools, roads or electrical power plants - and of population must
130 be procured at component (i.e. asset) level for the area of interest, such as a country, state or greater
131 metropolitan area. Within the modelling framework, user-provided data sources may be ingested or high-
132 resolution data can be obtained via automatized queries from open-source data providers such as
133 OpenStreetMap and the WorldPop project [46]. A first step of complexity reduction and standardization
134 then consists in limiting the diverse structural components per CI network to a few main building blocks or
135 components. For instance, the road network could be reduced to intersections (nodes) and streets (edges),
136 without differentiating further between road types, bridges or tunnels (c.f Table B.1 for a non-prescriptive
137 component selection example for six main types of CI networks at various resolutions). Further, supply and
138 demand data of the CI networks and their end-users, e.g. electricity generation and consumption statistics
139 for the power network, as provided by the International Energy Agency (IEA), may be collected as available.
140 This is, however, not imperative for the presented approach, as will be demonstrated throughout the
141 method sections.

142 As a stylized example throughout the remainder of the model description, we consider the mobile
143 communication (c), electric power (e) and health (h) networks represented through their most crucial
144 components (respectively, cell towers, power plants, transmission lines, poles, and hospitals) and
145 population grid cells (p) representing end-users as illustrated in Figure 2.2, panel BS.1. Fictitious power
146 plant generation values and per capita electricity consumption statistics are included to demonstrate a
147 case of demand and supply data availability, whereas such statistics are here supposed to be unavailable
148 for all other CI networks.

149 **2.1.2. Graph Representations**

150 Infrastructure components are hence transformed into directed graphs consisting in nodes and edges.
151 Within the modelling framework, corresponding cleaning and conversion algorithms are provided. In our

152 example, the power network's plant and poles are represented by nodes and power lines as edges, while
153 the graphs for communication and healthcare networks are made up of nodes only (see Figure 2.2, panel
154 BS.1 (centre)). These formal representations will henceforth be referred to as *CI graph* G^j , where j is the
155 system type (e.g. G^e for the electric power CI graph). In addition, geographical location L , initial functional
156 state F^0 and the infrastructure-specific damage threshold D^j are set as attributes for all elements (nodes
157 and edges) in each CI graph. F^0 is set to 1 for all elements. D^j indicates the structural damage fraction
158 beyond which a component will lose its functionality and is a simplifying concept to derive functional states
159 from damages. Thresholds are set arbitrarily in this example for purely illustrative purposes. The population
160 network similarly is represented by a node-containing graph with people counts and geographical location
161 as node attributes.

162 **2.1.3. Dependency Heuristics**

163 Departing from an extensive review on CI interdependence models, a list of 120 functional and logical
164 dependencies between components of 11 different CI networks was collected (see Supplementary
165 Materials) and consolidated within six generic rules, referred to as *dependency heuristics*:

- 166 I. Most CI networks depend on electric power supply, (cooling) water supply and information and
167 communications technology (ICT)
- 168 II. People-hosting facilities (e.g. hospitals, schools, power plants) depend on road access
- 169 III. Dependencies can be categorized into either having redundant character, where several sources
170 can provide necessary support (e.g. telecommunication access from any reachable cell), or being
171 unique, where support is provided from a unique source (e.g. power from the single closest power
172 line).
- 173 IV. Dependencies are distance-constrained (e.g. a cell tower located 500 km away will not provide
174 relevant service, neither will a hospital which is 1500 km across the country).
- 175 V. Dependencies may entail a continuous, physical flow between source and target (e.g. water,
176 electricity), yet can be approximated through a binary, logical connection.
- 177 VI. Population (end-users) depends on CIs for services, but not vice-versa.

178 These rules serve as a first starting point to identify sets of CI networks between which functional
179 dependencies likely exist, and to sketch out a set of variables which can be fed into a quantitative
180 dependency-search algorithm: *source*, *target*, *distance threshold*, *redundancy*, *road access* and *flow*. These
181 dependency-search variables, described in more detail in Table 2.1, can be parametrized and manually
182 adjusted to the case study at hand. The modelling framework's algorithm then places directed edges e^{jk}
183 (dependencies) between any nodes of CI graph pairs (G^j, G^k) which fulfil the dependency conditions
184 specified in the parametrizations of the described variables. In the stylized example of Figure 2.2, panel
185 BS.1 ('Interdependent CI Graph'), a dependency list indicates CI network pairs which are generally
186 hypothesized to exhibit dependencies (white underlaid). For instance, hospitals (target) are likely

187 dependent on electric power (source), which for hospital node 6 is supplied uniquely from power node 3
 188 (no redundancy), given that the supply point was close enough (distance < distance threshold).
 189 The dependency-search algorithm equally allows assignment of end-users to CI networks in the absence of
 190 more detailed, yet often proprietary utility providers' customer data; the population graph is then the
 191 target of infrastructure - end user pairs (G^j, G^p) for any relevant infrastructure type j . The algorithm hence
 192 results in the creation of one *interdependent CI graph* G from all CI graphs and the population graph. This
 193 is illustrated in Figure 2.2, panel BS.1 ('Interdependent CI Graph'); population cluster node 12 (source), for
 194 instance, is dependent on any (redundancy) of the cell towers (target) within the set distance threshold for
 195 the provision of mobile communications, which is fulfilled by cell tower node 12.

196 *Table 2.1 Required variables for the dependency-search algorithm between CI graphs. 'Source' and 'Target' are CI network*
 197 *components of different systems, previously identified from the heuristics explained above. Specific values for the variables*
 198 *may be filled in as adequate for the case study at hand.*

Variable	Description
Source	Supporting CI component
Target	Dependent CI component
Distance Threshold	The maximum distance for establishing a link between two nodes is determined by a circle around the target with respective radius if road access is not required, else the shortest path via road edges connecting source and target nodes must not exceed the specified threshold.
Redundancy	Whether a target node is connected to all CI nodes of type source within a specified distance threshold (<i>TRUE</i>) or only to the single closest one (<i>FALSE</i>).
Road Access	Whether a road path must exist between source and target.
Flow	Whether the flow through the dependency edge is informed by a physically informed, continuous variable (' <i>physical</i> ', such as power cluster capacity), or by a binary (' <i>logical</i> ') variable, indicating if supply can be provided or not based on the functional state of the source.

199
 200 Next, for each combination of source-target pair jk for which edges e^{jk} were created in the interdependent
 201 CI graph, the attributes capacity C^{jk} and capacity threshold T^{jk} are assigned to all nodes. C^{jk} is initialized to
 202 discrete values, depending on whether a node is a source (1), a sink (-1) or neither (0) for the flow from CI
 203 network of type j to type k . T^{jk} $([0,1])$ indicates what percentage of a standardized flow unit from j needs
 204 to arrive at a component of type k for it to remain functional. Bespoke hospital node 6 in Figure 2.2, panel
 205 BS.1 ('Interdependent CI graph') depends on electric power (e) and telecommunications (c), and provides
 206 healthcare services to people (p), and hence C^{eh} and $C^{ch}=-1$, while $C^{hp}=1$. For the hospital to remain
 207 functional in this example, it needs to receive at least 0.6 standardized units of power through its
 208 dependency link(s) ($T^{eh}=0.6$), 1 unit of telecommunications access ($T^{ch}=1$), and no unit of healthcare access,
 209 since it is the provider of this service ($T^{hp}=0$).

210 Geographic dependencies [13], [20] are implicitly accounted for in the framework through the spatial
 211 explicitness of all representations.

212 2.1.4. Flow Assignments and Infrastructure Functionality

213 Incorporating commodity flows in addition to a system's topology has been argued as crucial for capturing
 214 system performances adequately [31]. Yet, interdependent CI networks entail flows *within* individual
 215 networks (e.g. power in the power grid), and *across* networks (e.g. power to hospitals). Flows are
 216 furthermore of different natures, involving physical commodities (water, electricity, etc.) as well as logical

217 dependencies (connectivity to mobile communications). To deal with this diversity, internal flows in CI
218 networks and flows along dependencies between CI networks are treated separately. Results are then
219 translated into binary functional states and normalized capacity values for coherence across all networks.
220 Formally, those calculations are performed on subgraphs of the previously established interdependent CI
221 graph G , henceforth denominated as G^j and G^{jk} . Subgraphs span all elements of infrastructure type j , and
222 of types j, k , and linking edges e^{jk} , respectively, yet also retain their reference to the overarching graph G ,
223 which is hence updated. Figure 2.2, panel BS.2 provides a visual illustration of such subgraphs.

224 **Flows within networks** For networks with internal flows between sources and sink elements,
225 infrastructure type-specific flow assignment algorithms, flexibly tailored to the data and knowledge
226 available, are employed to update all capacity attributes C^{jk} on the corresponding subgraphs G^j (for
227 examples on flow calculation approaches, see [47] for road networks, [48] for water networks and [49] for
228 power networks). Figure 2.2, panel BS.2 (left) illustrates this procedure for the power network, which is
229 the only network involving internal commodity flows in this stylized example. In absence of further system
230 knowledge apart from demand (per capita consumption data), supply (power plant generation data) and
231 network topology, a cluster approach is employed. For each cluster in G^{e} (here there is only one cluster),
232 the ratio of supply (28 GWh) to demand (35 GWh) is computed, and assigned as a new relative capacity
233 value C^{ek} (here 0.8) to all nodes in that cluster. This can be read as the power system operating at $C^*100\%$
234 of its required capacity. Functional states F of the components remain unaltered in this mechanism.

235 **Flows across networks** The goal of this step is to determine the functionality F of each dependent
236 infrastructure node in the interdependent CI graph based on the available capacities from other supporting
237 infrastructure nodes. For each unique type of dependencies jk (e.g., power-communication, $j=e, k=c$) in G ,
238 subgraph G^{jk} is extracted. A received supply variable M^{jk} is computed for each node in G^{jk} . M^{jk} amounts to
239 the sum of capacities C^{jk} received at target nodes k from functional source nodes j via an edge e^{jk} , and is
240 hence 0 at nodes of type j . Technically, this flow propagation is computed on the adjacency matrix using
241 matrix multiplication only, which is computationally efficient even for large networks. If M^{jk} is smaller than
242 a previously set capacity threshold T^{jk} , a node loses functionality ($F=0$). Figure 2.2, panel BS.2 (right)
243 illustrates this procedure formally (Eqs. (1) and (2)) and graphically on the electric power-mobile
244 communications subgraph, which entails a physical, continuous variable flow, and on the mobile
245 communications-healthcare subgraph, approximated by a binary (logic) variable flow: The cell tower node
246 #7 receives a total of $M^{ec} = 0.8$ normalized units of power from the power sources it is connected to, which
247 is greater than the capacity threshold (here set to $T^{ec} = 0.6$). It hence remains functional ($F=1$). Hospital
248 node #1 receives $M^{ch} = 2$ logical units of supplies from both cell towers it is connected to. As this exceeds
249 the needed (logical) units of cell tower supply ($T^{ch} = 1$), the hospital also remains functional ($F=1$).

250 Since dependency loops (inter-dependencies) can exist among CI networks, internal and inter-network flow
251 assignment procedures are iteratively repeated until there are no more functional variable changes across
252 any elements in the interdependent CI graph G .

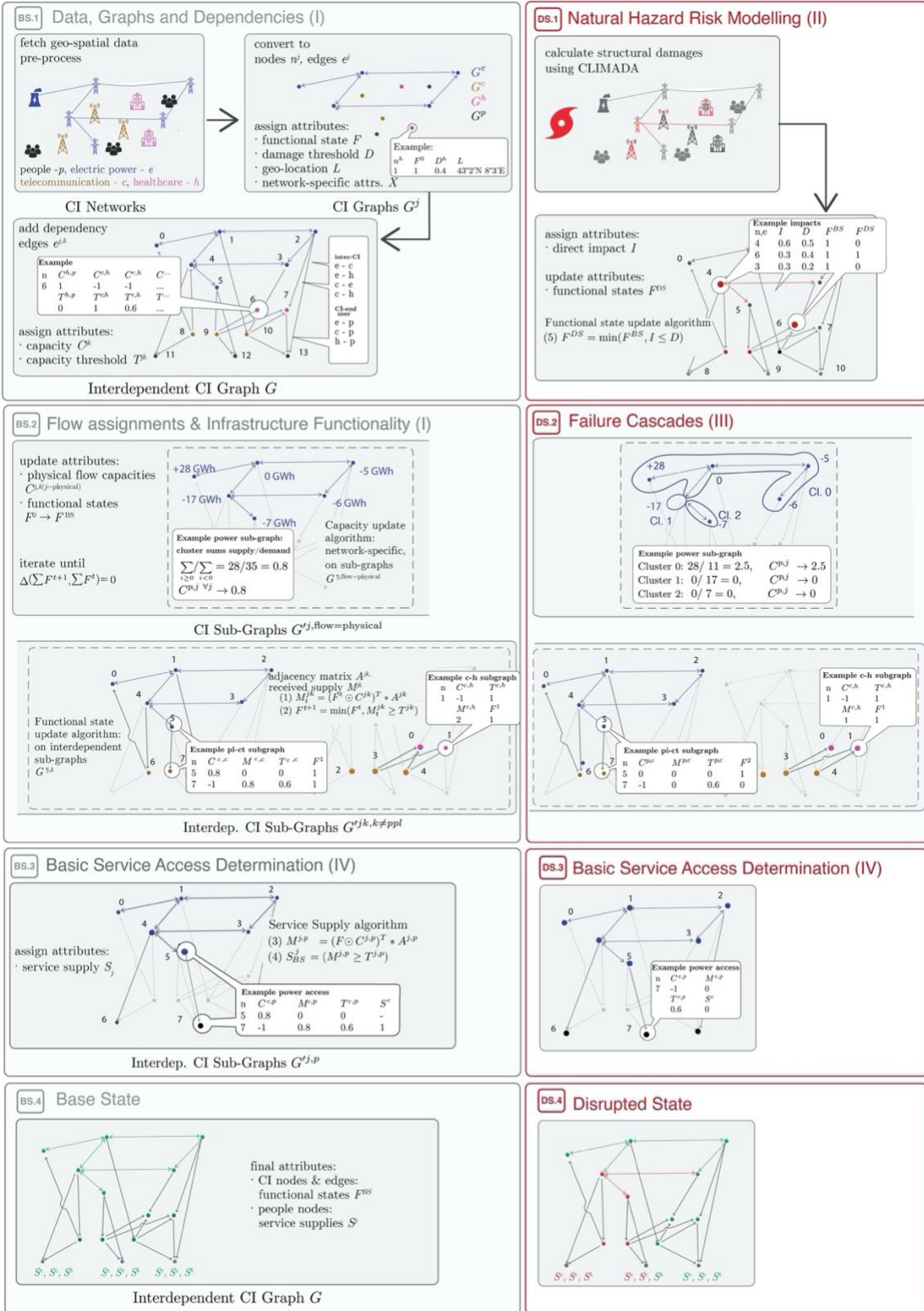


Figure 2.2 Stylized illustration of the entire modelling chain for 3 CI systems, people and a tropical cyclone event. Panels BS.1-4 (left) show the setup of the infrastructure systems model given infrastructure data, population data and dependency heuristics (BS.1), flow assignments and infrastructure functionality determination (BS.2), and basic service access determination for the population (BS.3), which hence represents the base state of the system (BS.4). Panels DS.1-4 (right) demonstrate the effects of structural damages caused by a natural hazard event (DS.1) triggering CI failure cascades (DS.2) and causing basic service disruptions to the population (DS.3). Roman numbers in brackets refer to the corresponding stages in overview Figure 2.1. Detailed explanation is given in sections 2.1 - 2.4. For a list of abbreviations and formal treatment, see annex A.

254 **2.2. Stage II: Natural Hazard Risk Model**

255 While several platforms for natural hazard modelling exist, the open-source and -access software CLIMADA
256 (CLimate ADAPtation) [45] is the only globally consistent and spatially explicit tool which is freely available
257 to assess the risks of natural hazards and to support the appraisal of adaptation options [50]. The event-
258 based modelling approach of CLIMADA has been used, among others, to conduct risk studies of tropical
259 cyclones on assets across the globe [51], to discern impacts from river floods in a changing climate [52] and
260 on people displacement [53], and in the wider context of Economics of Climate Adaptation studies [54].
261 The framework allows for a fully probabilistic risk assessment based on the IPCC risk definition [55] as a
262 function of hazard, exposure and vulnerability.

263 **2.2.1. Hazard**

264 *Hazard* is a spatially explicit representation of the intensity of a natural physical event, such as geo-
265 referenced wind speed for storms or water height for floods. Hazard footprints can, for instance, be based
266 on historic records, forecasts or climate projections, or be synthetically generated to create probabilistic
267 event sets. In CLIMADA, hazard modules are available for tropical cyclones, floods, wildfires, earthquakes,
268 landslides, avalanches and heatwaves in different stages of maturity, yet can also be provided through
269 user-ingested raster or vector data.

270 **2.2.2. Exposure**

271 *Exposure* refers to the geo-referenced assets or population data that are located in the area of interest. In
272 CLIMADA, exposure modules are available to retrieve a global gridded asset dataset (LitPop [56]), critical
273 infrastructures from OpenStreetMap, and high-resolution gridded population data out-of-the-box. User-
274 provided data in raster or vector formats can equally be ingested. Exposures require a value assignment
275 to capture the value potentially at risk, such as pre-computed economic (Dollar) values for LitPop, and
276 lengths, areas or simply unity for infrastructure components (e.g. 100 m for a road section or 1 for 'a'
277 healthcare facility).

278 **2.2.3. Vulnerability**

279 *Vulnerability*, also termed *impact function* or *fragility curve*, is an exposure-specific mapping of hazard
280 intensity to expectable damage extent. Vulnerability curves for tropical cyclone winds on general economic
281 asset stocks have been calibrated in CLIMADA for nine world regions [57], while the dedicated impact
282 function module also allows to specify hazard- and infrastructure-component specific functions taken from
283 literature, such as the HAZUS technical manuals provided by the US Federal Emergency Management
284 Agency (FEMA).

285 **2.2.4. Risk (Structural Damages)**

286 Risk calculations are performed in CLIMADA by spatially overlaying hazard and exposures and mapping
287 impacts via the corresponding impact function. Since most infrastructure exposures originally come in line
288 or polygon formats, such shapes are interpolated to centroids at user-defined resolutions, and re-
289 aggregated into their original shape after impact calculations. Here, risk is hence measured in terms of

290 estimated structural damage to all infrastructure exposures, which in turn is expressed according to the
291 respective value metric (either as damage fraction or total length/area affected). Computed structural
292 damage values are then assigned as attribute I ('*impact*') to each corresponding element in the
293 interdependent CI graph G . See Figure 2.2 panel DS.1 for an illustration of tropical cyclone risk calculations
294 on power lines, cell towers and healthcare facilities.

295 **2.3. Stage III: Technical Impacts (Infrastructure Failures)**

296 For each element in the interdependent graph, the impact to the corresponding component computed
297 with CLIMADA is assigned as attribute I . Functional state F of an element is set to zero if the impact I exceeds
298 the damage threshold D^j as illustrated in Figure 2.2, panel DS.1.

299 This change in functional states can set off a failure cascade within the graph, through both internal and
300 dependency-induced flow changes. In order to propagate the disruption, the capacities and functional
301 attributes of all CI components are updated by applying the algorithm described in section 2.1.4 iteratively
302 until a new steady state is obtained. In our example illustrated in panel DS.2 in Figure 2.2, several cascades
303 occur: The power graph is split into three clusters as a consequence of the initial failure of a node and an
304 edge element, whereby two clusters (Cl. 1 and Cl. 2) remain without capacity as they are cut off from
305 connection to the power plant ($C^{ek}=0$). Interdependencies among CI networks further propagate those
306 disruptions (cell tower #7 is connected to a capacity-less power node, hence becoming dysfunctional;
307 hospital #1 still receives 1 unit of supply - instead of previously 2 - from supporting cell towers, which
308 prevents its failure).

309 **2.4. Stage IV: Human-centric Impacts (Basic Service Access & Disruptions)**

310 The final step is to compute basic service access (and disruptions, correspondingly) for a range of services
311 at population nodes. Basic service access, according to the United Nation's definition¹, is ensured through
312 the confluence of two factors:

- 313 i. *functionality* of the CI (component) responsible for the provision of a service
- 314 ii. a notion of *accessibility* to the CI (component)

315 Here, we define functionality through the functional states of the infrastructure graph elements.
316 Accessibility is defined either through literal road path availability between end-user and infrastructure
317 (e.g. hospitals for healthcare services) or through coverage of an area around an infrastructure's location
318 (e.g. cell towers for mobile communication services). A qualitative summary of basic service access
319 parametrizations for six services examined in this work is given in Table 2.2.

320

¹ Metadata repository to the SDGs for indicator 1.4.1 - Proportion of population living in households with access to basic services: "*Basic Services refer to public service provision systems that meet human basic needs including drinking water, sanitation, hygiene, energy, mobility, waste collection, health care, education and information technologies. [...] Access to basic services implies that sufficient and affordable service is reliably available with adequate quality.*"

321 *Table 2.2 Examples for basic service access conditions which can be implemented in the infrastructure system model.*

Basic Service	Description
Mobility	Functional connection to an intact road element within a certain distance threshold.
Power	Functional connection to an intact power cluster which runs above a certain capacity ratio.
Healthcare	Existence of an intact road-path below a certain distance threshold to a functioning facility.
Education	Existence of an intact road-path below a certain distance threshold to a functioning facility.
Mobile communication	Functional connection to an intact cell tower within a certain distance threshold.
Drinking water	Functional connection to an intact wastewater treatment plant within a certain distance threshold.

322

323 The quantitative basic service access algorithm is implemented in analogy to the flow assignment and
 324 functionality determination algorithm in the previous step. For each unique infrastructure-population pair
 325 combination jp , for which dependency edges e^{jp} exist in the interdependent CI graph G , the subgraph G^{jp}
 326 spanning G^p , G^j and e^{jp} is extracted. Received services M^{jp} are hence computed as the sum of capacities
 327 from source infrastructure nodes arriving at population nodes (see eqs. 3 and 4 in Figure 2.2, panel BS.3).
 328 Each population (target) node is then assigned a service attribute S^j , indicative of the service provided by
 329 CI type j . The service is accessible ($S^j=1$) if M^{jp} exceeds the capacity threshold T^{jp} and, additionally, fulfils the
 330 access conditions (c.f. Table 2-3), else $S^j=0$. While the coverage-based access conditions are implicitly
 331 accounted for through the (non-)existence of a dependency edge, the literal (road-access) condition is
 332 checked for explicitly in the interdependent CI graph G through a shortest path algorithm, calculating the
 333 distance of the path between population node and facility node. Panel BS.3 in Figure 2.2 illustrates the
 334 procedure with the example of electric power access, where population node #7 receives $M^{ep}=0.8$
 335 normalized units of power, which exceeds the capacity threshold ($T^{ep}=0.6$) and hence the service is
 336 accessible ($S^e=1$).

337 The interdependent CI graph with functional state attributes F at infrastructure elements and service
 338 attributes S at population nodes hence defines the *base state*. Panel BS.4 in Figure 2.2 illustrates this for
 339 the three infrastructure networks and the corresponding three service types at the population network
 340 (electric power access S^e , basic information access S^c and healthcare access S^h).

341 Once CI component failures are determined, basic service access is re-computed as hence described. See
 342 illustration in panel DS.3 in Figure 2.2 for the given stylized example on population's power access, leading
 343 to a new, *disrupted state* (panel DS.4 in Figure 2.2).

344 **2.5. Model Uncertainties and Sensitivity Testing**

345 Due to the amount of consecutive stages featured in the presented modelling chain, model assumptions
 346 and representational choices in one stage may greatly influence end-results. In order to allow for
 347 evaluation of such sensitivities, Table 2.3 provides a brief discussion on the main points where model
 348 uncertainties are introduced.

349

350

351 *Table 2.3 Drivers of model uncertainties throughout all stages in the modelling chain.*

Stage	Source	Explanation
I	CI system representations	Choices on CI components included or excluded, simplifications (for instance, no differentiation between transmission lines of different voltages, approximating the communication network by cell towers, water network by water treatment plants)
	Dependency Identification	Choice of dependency rules (i.e., heuristics, between which CI systems dependencies exist)
	Dependency Parametrization	Choice of conditions for dependency establishment (i.e. distance thresholds between components identified through heuristics, path requirements, etc.)
II	Hazard Footprint	Resolution, spatial accuracy and representational validity, when in- or excluding sub-hazards (e.g. wind-fields, storm surge and torrential rainfall for tropical cyclones) or multi-hazard phenomena (compound events).
	Vulnerability Curves	Assumptions on (deterministic) relationship between hazard intensity and component damages.
	Damage-Functionality Thresholds	Assumptions on the (deterministic, threshold-based) relationship between structural damages and resulting component functionality levels.
III	Cascading algorithm	Deterministic (strict) propagation of failures along dependencies, assumption on target becoming strictly dysfunctional due to failure at source.
IV	End-user Dependencies	Uncertainties are analogous to stage I.
	Basic Service Parametrization	

352
 353 Owing to the complexity of the presented approach, a one-at-the-time analysis obtained by constructing
 354 scenarios, where only one set of parameters are varied within plausible bounds at a time (such as
 355 parametrizations of dependency conditions, vulnerability curves and functional thresholds), is a good
 356 starting point for identifying key sensitivities in the system responses. More in-depth characterization of
 357 the uncertainties can then be carried-out by focusing on the identified sensitivities (see [58] for a
 358 comprehensive discussion on best practices and recommendations, catering specifically to the field of
 359 environmental modelling, and [59] for an exemplary computational workflow designed for uncertainty
 360 propagating in and multi-level sensitivity analysis of hierarchical systems, particularly interdependent CI
 361 networks). Much can be done directly in CLIMADA using the ‘*unsequa*’ module that provides readily usable
 362 methods for state-of-the art global uncertainty quantification and sensitivity analysis based on quasi-
 363 Monte Carlo sampling [60]. In addition, the probabilistic hazard modelling approach may help estimating
 364 representational uncertainties on the trigger side.

365 **3. Application: CI Failures and Basic Service Disruptions from Hurricane Michael**

366 Tropical Cyclone Michael made landfall in the Florida Panhandle on the 7th of October 2018, and caused
 367 severe impacts across Florida, Alabama and Georgia, both in terms of direct asset damages (over US\$ 25
 368 billions) and lives lost (at least 43) [4], as well as in terms of CI failures (power and mobile communication
 369 outages affecting millions, among others). It was selected for demonstration based on two reasons. Ample
 370 documentation of the event permits result validation and provides a reality check on quality and
 371 information content of the developed model. Further, Michael’s severity was dominated by strong winds
 372 and storm surge as opposed to torrential rainfalls [61]. The hazard can therefore be approximated by
 373 modelling only its wind-field, lending itself as an illustrative, yet simple enough example.

374 **3.1. Model demonstration**

375 **Stage I: Infrastructure System Model (Infrastructure Functionality)** We delimit the system of
376 study to the states of Florida, Alabama and Georgia which were directly hit by hurricane-strength winds.
377 Besides population, infrastructure systems considered are main roads, transmission power lines, power
378 plants, cell towers, wastewater treatment plants, healthcare institutions and public schools (see Figure 3.1
379 column 'CIs' for geographical maps of the CI networks). Details on data sources, pre-processing and
380 individual CI graphs generation, can be found in annex C.1.1. Generation sources and demand sinks within
381 the power network are obtained from power plant generation and energy consumption statistics (annex
382 C.1.2). To generate the interdependent CI graph, twelve distinct dependencies are identified in between CI
383 networks (6) and between CI networks and population (6), and parametrized as indicated in annex C.1.3.
384 The established interdependent CI graph consists of nearly 80'000 nodes and 500'000 edges, with
385 dependencies making up the majority (59%) of links (see Figure C.1 for detailed graph statistics). Network
386 flows are computed and functional states assigned to all infrastructure components in this pre-disaster
387 configuration (termed 'base state'), resulting in all elements of the interdependent CI graph being
388 functional. Population's basic service access rates surpass 99% for all service types considered in the base
389 state (access to mobility, power, education, healthcare, mobile communications and drinking water).

390 **Stage II: Natural Hazard Risk Model (Structural Damages)** Track data for tropical cyclone Michael
391 is obtained from the International Best Track Archive for Climate Stewardship (IBTrACS) project [62]. The
392 wind field (see Figure C.2) is computed from the CLIMADA tropical cyclone module, according to the
393 parametrization in [63]. CI-type specific impact functions for structural damages from winds are taken from
394 literature (see annex C.2.2) and ingested into CLIMADA for all infrastructures except power plants, which
395 are not designed to fail. All CI networks are converted to CLIMADA exposure layers for impact calculations.
396 Structural damages are computed using the CLIMADA impact module, yielding direct impact figures as
397 displayed in Figure 3.1, column 'Component Damages'.

398 **Stage III: Technical Impacts (Infrastructure Failures)** Structural damages fractions of all
399 infrastructure components are translated into binary functionality states by applying infrastructure-specific
400 threshold values (annex C.1.3). Component failures hence initiate the failure cascade algorithm in the
401 infrastructure systems module, both within individual CI networks and along dependencies across CI
402 networks. Under the given system specifications, only the power network features an internal cascading
403 mechanism, as it contains designated source nodes (power plant), sink nodes (power line nodes with
404 customer demands) and transition nodes (all other power line nodes). A cluster approach was chosen to
405 capture this failure behaviour, where all components in a remaining functional cluster become
406 dysfunctional once generation capacity falls below a certain fraction of demand (here set to 60% for
407 demonstrative purposes). Dependency-induced failure cascades are experienced across all CI networks
408 within the interdependent CI graph. Results are displayed in Figure 3.1, 'CI failures', where initial, structural
409 damage-induced failures and cascaded failures are marked with the respective colour code.

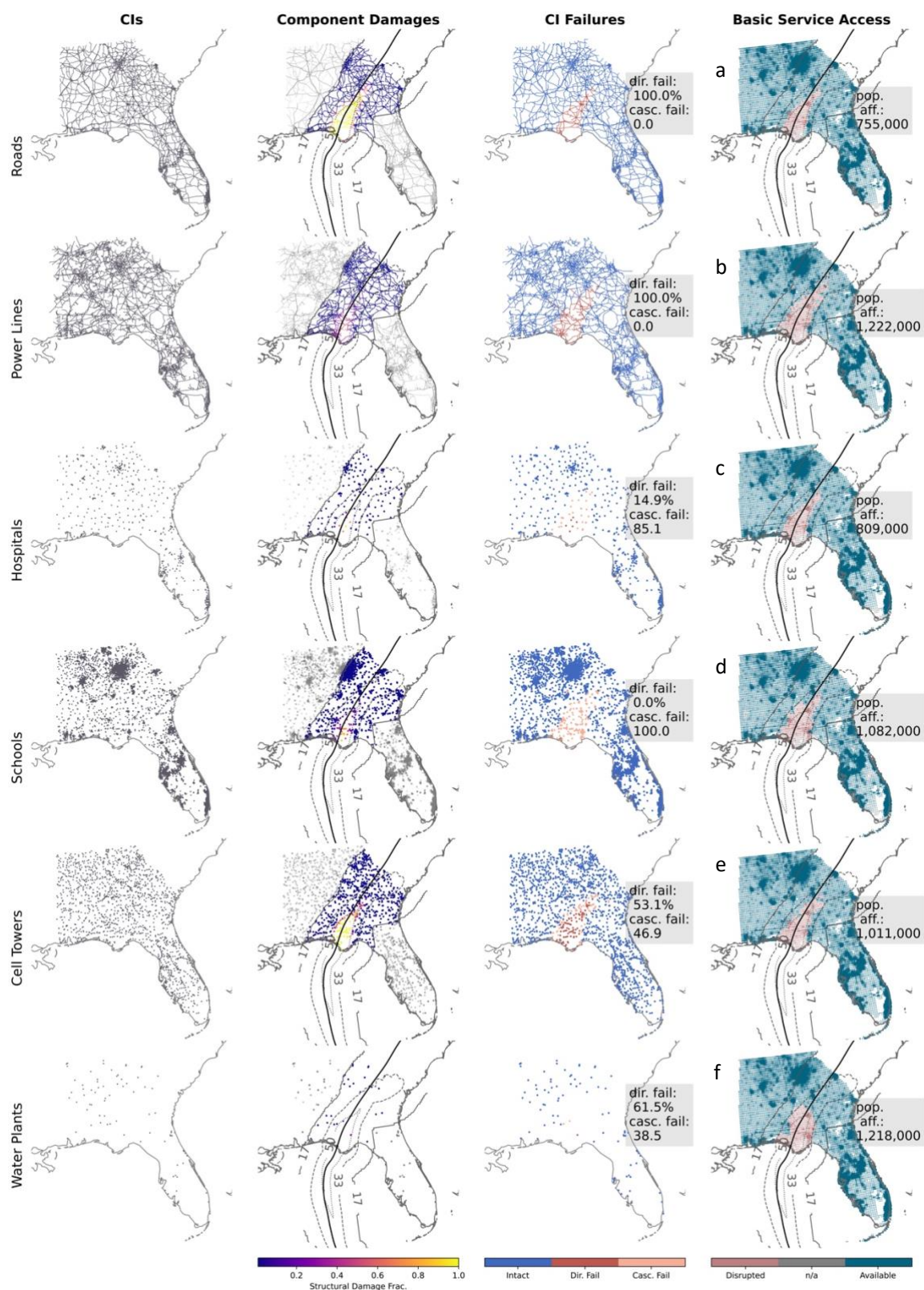


Figure 3.1 From natural hazard to basic service disruptions in four stages. Demonstration for Hurricane Michael '18 hitting the Florida Panhandle: Asset data for 6 CIs across FL, AL & GA used in the CI model (column 'CIs'), wind-induced structural damages calculated with CLIMADA ('Component Damages'), CI failure cascades triggered by the initial disruption, resulting in functional, dysfunctional and cascaded dysfunctional components ('CI failures'), population impacted from basic service disruptions following CI failures ('Basic service access', a: access to mobility, b: power, c: healthcare, d: education, e: mobile communication, f: drinking water. TC track and wind-field contour lines (m/s) are plotted in columns 2 & 4 for reference.

411 **Stage IV: Human-centric Impacts (Basic Service Disruptions)** Following the failure cascade
412 algorithm, access to basic services are computed for all population nodes within the interdependent CI
413 graph. For road-path constrained dependencies (access to healthcare and education, resp.), this involves
414 re-calculation of path availability and travel distances. Figure 3.1, 'Basic Service Access' shows the
415 disruption results for access to mobility, power, healthcare, education, mobile communication and drinking
416 water.

417

418 **3.2. Scenario Analysis**

419 To obtain first insights on how strongly results depend on assumptions along the modelling chain, seven
420 modelling scenarios are constructed (see Table C.4). We explore the role of interdependencies, and of
421 parametrization decisions for impact functions and for functionality thresholds on result outcomes (annex
422 Table C.5 for numeric results). The above presented case, referred to as 'original' parametrization
423 henceforth, is taken as a reference.

424 Results are greatly influenced by the inclusion of CI interdependencies: As cascaded failures account for a
425 significant part of all infrastructure failures in the base scenario, the removal of this impact driver drastically
426 reduces component failures across all CI types but roads, with strong consequences for projections of
427 service disruptions. Numbers of affected people decrease for all basic services apart from access to mobility
428 (see Figure 3.2, blue). While the inclusion of dependencies itself plays a great role in determining the
429 magnitude of impacts, the exact parametrizations of establishment conditions thereof (such as path
430 distance thresholds) affect end results less strongly (see Figure 3.2, reds). Parametrization of impact
431 functions directly and strongly influences estimates of structural damages, which has far-reaching
432 consequences on the entire impact chain from immediate CI failures over cascades to basic service
433 disruptions. Shifting impact functions by 15 m/s in either direction compared to the base scenario (i.e.
434 same level of structural damage at wind intensities of 15 m/s more or less, resp.) can lead to a divergence
435 in services disruption estimates between millions of people and almost none (Figure 3.2, greens).

436 Due to the resolution of the hazard footprint (360 arcsec, ca. 11 km), which exceeds most CI component
437 lengths, results are less sensitive to the threshold assumptions between structural damage fractions and
438 functional performance of components, since components are mostly entirely affected or not at all (see
439 Table C.5). This may change and become increasingly important, though, at higher hazard resolutions.

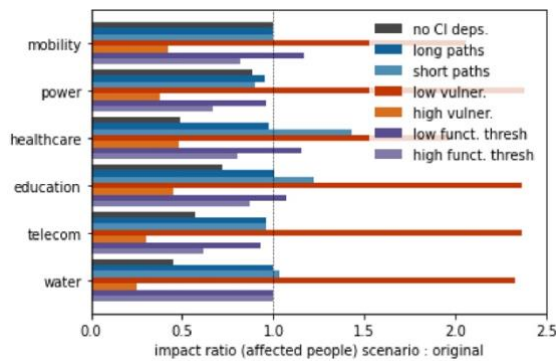


Figure 3.2 Number of people affected by basic service disruptions for seven scenarios, relative to original parametrization presented in section 3.1. Blue: no CI interdependencies, reds: allowing for shorter and longer road travel paths to social facilities, greens: higher and lower CI component vulnerability, greys: higher and lower structural damage thresholds until reaching component dysfunctionality.

441

442 **3.3. Validation**

443 The aim of this validation is to collect evidence on whether the showcased impact cascades - from CI
 444 damages to affected people - *do* happen, and whether predicted impacts, even when drawing on coarse
 445 assumptions and a set of heuristics, are in the right order of magnitude. The multiple impact stages
 446 calculated within the underlying approach are reflected in the breadth of validation sources taken into
 447 account, and span official government releases, utility providers' reports and newspaper articles (see annex
 448 C.4 for a comprehensive overview).

449 Even for the case study region, where information sources after natural hazard events are ample and
 450 accessible, documentation on the entire impact cascade is incomplete: structural damages are only
 451 incidentally reported across all infrastructure types, comprehensive functional outage reports are limited
 452 to the power and telecommunication sector, while accounts on basic service disruptions remain anecdotal.

453 Figure 3.3 synthesizes this evidence, contrasting quantitative outage statistics against model outputs
 454 (panels b and e for power and telecom), and mapping qualitative service-related incidents against areas of
 455 modelled access disruptions (panels a, c, d and f for healthcare, education, mobility and drinking water).

456 Loss of power access is captured well, both in terms of impacted people (~1.65 million reported vs. 1.22
 457 million modelled), and in terms of spatial distribution (compare Figure 3.1 and Figure 3.3 (a) for a more
 458 detailed visual reference). Loss of mobile communication access is not reported as such, yet documented
 459 occurrences of cell site outages coincide well with spatial model predictions on failed cell towers (see Figure
 460 3.3 (e), aggregated at county level); most county predictions lie well within a 50% margin of error, even
 461 though the impact severity is overestimated in hurricane-hit counties located further inland.

462 Documented incidents related to the loss of service access and infrastructure damages, such as hospital
 463 evacuations, structural damages and fatalities due to untimely care in the case of healthcare access, all lie

464 within the modelled area of concern (Figure 3.3). Yet, road damages and mobility-related incidents were
465 reported far less inland than model predictions (Figure 3.3 (a)), a tendency which is less pronounced, yet
466 shared for access to healthcare and education (Figure 3.3 (c, d)), and most drastic for evidence on drinking
467 water issues (Figure 3.3 (f)). The divergence in projected and actual disruptions to mobility confirms the
468 importance of choosing adequate impact functions, as pointed out also in the section on scenario analysis.
469 The road impact function used in this study was designed for disruptions from tree blow-down, which may
470 have provided an overly pessimistic picture on (longer-lasting) structural damages.

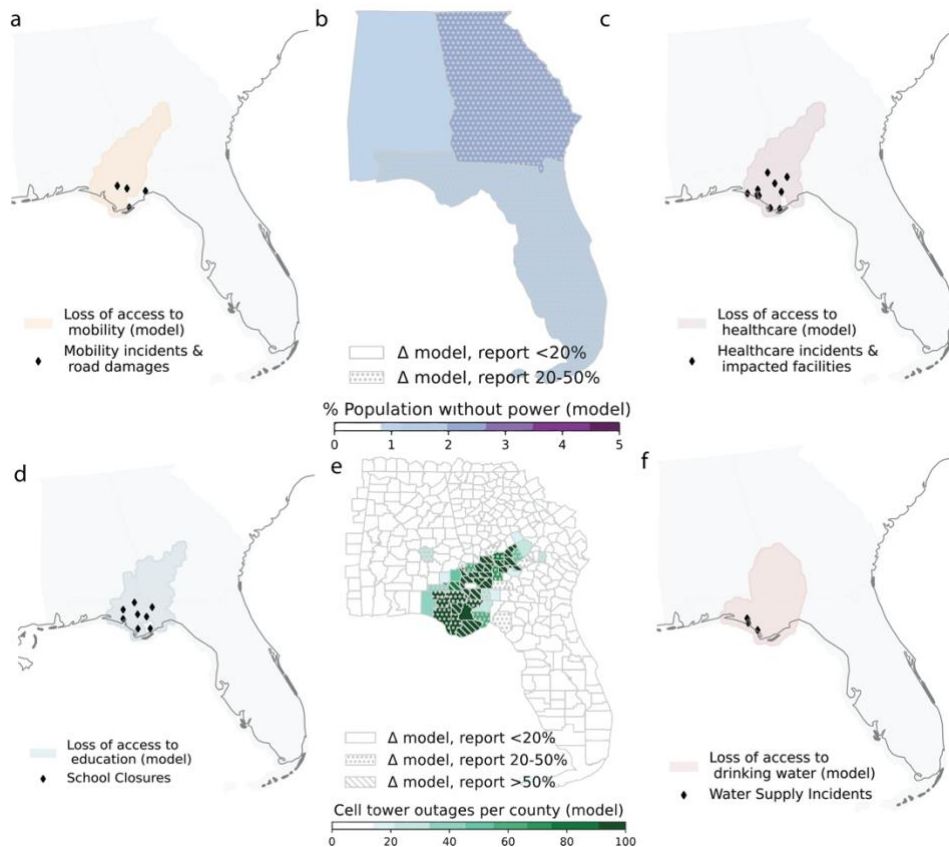
471 Validation results for mobile communications, healthcare and education access highlight the importance
472 of incorporating dependencies and failure cascade into the model, yet also show caveats of adequate
473 parametrization: The relatively accurate projection of people affected by cell site outages could not have
474 been reproduced without power interdependencies, as the scenario analysis showed above. Similarly,
475 several hospitals which were not directly damaged reported evacuations due to water and power supply
476 issues, while many of the indirect deaths were linked to either patients or emergency workers not getting
477 physical access to healthcare facilities in time. This confirms the general validity of incorporating such CI
478 dependencies into infrastructure functionality calculations, and the importance of people's road path
479 availability into bespoke service access computations. Such dependency specifications can, however, also
480 propagate errors and over-estimate disruptions, as seen with access to education: The estimated 45'000
481 students reported to be missing school due to closures [1] fall short of the approximately 145'000²
482 projected by the model. This is partly due to the non-redundancy between end-users and educational
483 facilities: Contrary to hospitals, where any facility within reach can be chosen, people are assigned to one
484 fixed school. When damages to such facilities or their supporting CIs are hence over-estimated, this will
485 transmit directly to over-estimations of education access disruptions throughout the entire assignment
486 surroundings.

487 Lastly, the case of water access disruptions demonstrates that a high degree of system simplification can
488 become problematic: In absence of better data, the drinking water system was proxied by water treatment
489 plants only. As a consequence, the model projected large areas of disruption from a single failing facility,
490 which seems not to be the behaviour observed in those real-world water systems. Similarly, caution should
491 be taken when approximating the telecommunications network - consisting in more and more resilient
492 sub-networks than mobile communication structures only - through cell towers.

493 Despite the fact that some service disruptions were less extensive than modelled, the integration of a
494 hazard model and a CI model based on relatively simple dependency heuristics and readily available open-
495 source data allowed to capture important failure dynamics within one interoperable calculation chain. The
496 model reproduces impacts in the correct order of magnitude, allows to trace back impact drivers to
497 parametrization decisions in each stage of the impact cascade, and to re-calibrate mechanisms. It further

² number of affected population corrected by by fraction of people enrolled in preK-12 (13.4%)

498 gives a social dimension to technical CI failures, mapping out areas of disruption for basic services which
 499 are not consistently monitored by official sources. While those are promising features, there is demand for
 500 an even more refined picture, as remarked by a reporter in the aftermath of TC Michael: “While the coastal
 501 devastation has become obvious, some disaster experts are most concerned about the conditions farther
 502 inland. [...] These are some of the most socially vulnerable places in the entire country, low-income
 503 counties with high proportions of older adults, and many people with disabilities and chronic illnesses”
 504 [64].
 505



506
 507 *Figure 3.3 Validation results for power outages (a), cell site outages (b), water supply issues (c), healthcare-access related*
 508 *incidents and hospital damages (d), road blockages, structural damages and mobility incidents (e) and school closures (f).*

509
 510 **4. Discussion**

511 The developed modelling framework was designed for interoperability, transferability and scale.
 512 Interoperability is achieved through the embedding of an infrastructure system model into the risk
 513 assessment platform CLIMADA, allowing for a streamlined workflow from natural hazards to social impacts.
 514 The linkage to an event-based hazard simulation engine is a way forward from the use of stylized polygons
 515 in absence of physically-informed hazard footprints [23], [65], hypothetical events [22] or return period
 516 maps which are not representative of individual events [66]. Transferability is ensured both theoretically
 517 and practically: While we provide readily available suggestions on infrastructure and population data
 518 sources, dependency heuristics, impact functions and hazard models, the framework can handle both

519 proprietary and/or other open-source data (e.g. regional or national-level developed data). This allows to
520 investigate other infrastructure types, hazards, dependencies and case study regions of interest to the user:
521 For instance, vulnerability functions may be altered to capture the important effect of deterioration
522 through ageing of infrastructures [67], or dependencies re-parametrized with different distance thresholds
523 to account for locally specific cell tower ranges [68] or travel speeds [69]. The scale criterion is integrated
524 in the design of the infrastructure system model, which requires few technical specifications, and relies
525 mainly on network topology and a set of heuristics for dependency and flow assignment procedures,
526 enabling the study of large systems.

527 The results simulated must be interpreted as a first indicator on impact hotspots and peak disruptions from
528 the angle of people at risk. The simplifying nature of network-based approaches has been recognized
529 earlier as a necessary trade-off against capturing large system scales at which natural hazards can occur
530 [18], [22]. The merit of the developed system model's approach therefore lies in the possibility of working
531 at a globally consistent basis with several interdependent CI systems, yet does not replace specialized
532 system models [31], [48], [49], [70] for detailed local analyses and individual infrastructure system
533 optimizations.

534 The three information levels on infrastructure risk which the model provides (structural component
535 damages, failure cascades, and service disruptions), align well with the highly diverse nature of real-world
536 impact data, which is often anecdotal and encompasses several of those risk layers. This offers the
537 versatility to calibrate and adjust parameters in the model based on evidence, such as tailoring impact
538 functions to match print media coverage on structural damages, or amending dependency heuristics to fit
539 utility provider's outage reports. To the best of our knowledge, only few quantitative modelling studies
540 [71] incorporate such feedback possibility. Obtaining results on direct and cascading infrastructure failures
541 further allows to quantify the role of infrastructure dependencies in causing wide-spread impacts:
542 Validation in the presented case study empirically confirmed that the extent of observed impacts could not
543 be reproduced without the inclusion of dependencies between infrastructure networks, which is in line
544 with findings from other research on infrastructure interdependencies [72], [73].

545 The scenario analysis highlighted that structural damage functions and dependency parametrizations are
546 sources of considerable uncertainties in the model. How to capture the diverse nature of
547 interdependencies, which adequately accounts for the varying 'coupling strengths' [13], [27] between CI
548 networks observed in reality, is a topic of ongoing research. The presented use of capacities, capacity
549 thresholds, redundancies and road-path availability checks in the parametrization of infrastructure
550 dependencies (annex A) is a pragmatic compromise between elaborate mathematical frameworks with
551 many conditionalities (for instance [74]) and implementation feasibility for large networks with limited
552 process knowledge and data availability. We refine commonly employed user-assignment procedures
553 relying purely on geospatial conditions (e.g. Voronoi tessellations) or on shortest path algorithms without
554 alternative targets [32], [43], [75]. Yet, modelling of back-ups for failing dependencies (such as generator

555 availability for power-dependent components [71]), changing demand patterns for infrastructure-related
556 services among end-users as a reaction to natural hazard occurrences [76], [77] or the reduction in
557 functionality as opposed to binary failures [74] upon dependency disruptions may improve currently
558 implemented cascading dynamics. Furthermore, the threshold approach employed to relate structural
559 damages to loss of component functionality is a simplification for the notoriously challenging task of
560 developing consistent performance indicators [27], [78], for which research in the engineering community
561 may lead to future insights.

562 Our approach does not feature an explicit notion of time. Since the modelled structural damages to
563 infrastructures need to surpass a certain threshold for the components to become dysfunctional, this
564 implies that the model captures rather longer-lasting disruptions. Yet, since impact severity is a function of
565 time and timing [79], making it an explicit variable can be insightful: While for healthcare access a few
566 hours of disruptions in the immediate aftermath of a natural hazard event may be extremely relevant, they
567 may be less so for access to schools, especially if occurring on a weekend. Introducing time could further
568 provide an informative indication on restoration and recovery dynamics [80], [81] when introducing repair
569 times and ‘snapshots’ of the interdependent CI network at various moments, and capture oscillating or
570 non-convergent functional behaviours which interdependent systems can exhibit.

571 Lastly, our estimates of post-disaster basic service disruptions add an often-neglected human-centric
572 dimension to the discourse on infrastructure risks [82], which both academic models, utility providers or
573 government post-disaster reports do not usually capture systematically (cf. [41] as a rare exception); the
574 holistic approach further allows to include under-represented sectors in CI research such as healthcare [42]
575 and education. This can offer valuable information to emergency responders with limited resources, and
576 decision makers facing multi-criteria investment decisions alike [41], [82], [83]. However, and especially as
577 research on social vulnerability is still in its infancy [39], it will be important to take a closer look at the
578 differential impacts of basic service losses on different parts of the population, such as the poor, the elderly
579 or non-native speakers, which have repeatedly been shown to dispose of fewer coping mechanisms [14],
580 [84].

581

582 5. Conclusion

583
584 Critical infrastructures such as powerlines, roads, telecommunication and healthcare systems across the
585 globe are more exposed than ever to the risks of extreme weather events in a changing climate. CI failure
586 models often operate at local scales with high data requirements and low transferability, focussing on the
587 technical performance side. Natural hazards are often not explicitly modelled as a disruptive scenario
588 therein. Natural hazard models, in turn, frequently focus on direct damages to assets, which neglect the
589 networked and interdependent character inherent to critical infrastructure systems.

590 To bridge those gaps between infrastructure modellers and natural hazard risk modellers, we draw on well-
591 established methods in both communities to develop an interoperable, coherent and open-source
592 modelling framework for assessing spatially explicit, large-scale risks from infrastructure failure cascades
593 and their social impacts induced by natural hazards. Embedded into the risk assessment platform CLIMADA,
594 a state-of-the-art tool for natural hazard impact calculations and adaptation options appraisal, we
595 demonstrate a network theory-based infrastructure systems model designed to require few technical
596 details apart from commonly available asset location and population data, which can handle many types
597 of infrastructure networks and captures interdependencies among them based on a set of heuristics. The
598 framework hence offers a three-layered view on infrastructure risks in terms of on infrastructure
599 component damages, technical failure cascades, and human-centric basic service disruptions. It is readily
600 transferrable across geographies, and can be tailored to include CI systems, interdependencies and hazards
601 of interest to the user.

602 The validated case study on Hurricane Michael across the US states of Florida, Georgia and Alabama for six
603 interdependent CI networks showed that the established modelling chain captures impact hotspots and
604 reproduces failure cascade dynamics, which could not be obtained when looking at structural
605 infrastructure damages alone. It also showed how real-world impact data, such as outage reports and print-
606 media accounts, can be used to iteratively refine and calibrate the model.

607 Projecting spatially explicit locations of service disruptions experienced by the dependent population as a
608 result of infrastructure failures further adds a novel layer of risk information, which is usually not available
609 on the ground.

610 While we do not offer the one single “comprehensive methodological approach with a platform of linked
611 models and data interoperability for modelling infrastructure interdependencies for a range of different
612 stakeholder concerns and decision contexts” [82] our approach takes a step into this direction. We provide
613 a tool apt for decision making-contexts involving large geographic scope and the effects of several
614 interdependent CI systems’ responses to disruptions for the population: The global consistency of the
615 approach permits a comparative view of risk across countries, relevant for international policy frameworks;
616 adaptation planning and infrastructure investments for resilience can be evaluated under their aversion
617 potential for different types of human-centric impacts and under trade-offs amongst different CI sectors;
618 post-disaster hotspot analyses can lead to more targeted humanitarian relief and recovery activities.

Acknowledgements

This project has received funding from the European Union's Horizon 2020 research and innovation programme under grant agreement No 821010 and under grant agreement No 820712. Elco Koks was further supported by the Netherlands Organisation for Scientific Research (NWO; grant no. VI.Veni.194.033).

Data Availability

CLIMADA risk assessment platform is accessible on GitHub (https://github.com/CLIMADA-project/climada_python for impact calculations, https://github.com/CLIMADA-project/climada_petals for the infrastructure system model). Code for reproducing case study results and figures is accessible under https://github.com/CLIMADA-project/climada_papers/tree/main/202208_critical_infrastructure_nw_risks. All raw data sources needed for reproducing calculations are mentioned in the text and annex.

References

- [1] W. T. Price and C. Glenn, "Schools closed across the Panhandle, 45,000 kids missing class due to Hurricane Michael," *Pensacola News Journal*, Oct. 17, 2018. Accessed: Jan. 25, 2022. [Online]. Available: <https://www.pnj.com/story/news/2018/10/17/hurricane-michael-closes-schools-florida/1660289002/>
- [2] Bay District Schools, "Hurricane Michael Recovery Information." <https://www.bay.k12.fl.us/hurricane-michael> (accessed Jan. 25, 2022).
- [3] J. Burlew, "43 and counting: Deconstructing the Florida death toll after Hurricane Michael," *Tallahassee Democrat*, Nov. 29, 2018. Accessed: Jan. 25, 2022. [Online]. Available: <https://www.tallahassee.com/story/news/2018/11/29/43-and-counting-deconstructing-death-toll-hurricane-michael/2124902002/>
- [4] J. L. Beven II, Robbie Berg, and Andrew Hagen, "Hurricane Michael Tropical Cyclone Report," National Hurricane Center, AL142018, May 2019. Accessed: Jan. 25, 2022. [Online]. Available: https://www.nhc.noaa.gov/data/tcr/AL142018_Michael.pdf
- [5] S. Thacker *et al.*, "Infrastructure for sustainable development," *Nature Sustainability*, vol. 2, no. 4, Art. no. 4, Apr. 2019, doi: 10.1038/s41893-019-0256-8.
- [6] McKinsey Global Institute, "Climate risk and response. Physical hazards and socioeconomic impacts.," Jan. 2020. <https://www.mckinsey.com/~media/mckinsey/business%20functions/sustainability/our%20insights/climate%20risk%20and%20response%20physical%20hazards%20and%20socioeconomic%20impacts/mgi-climate-risk-and-response-full-report-vf.pdf> (accessed Jun. 24, 2020).
- [7] A. N. Yesudian and R. J. Dawson, "Global analysis of sea level rise risk to airports," *Climate Risk Management*, vol. 31, p. 100266, Jan. 2021, doi: 10.1016/j.crm.2020.100266.
- [8] E. E. Koks *et al.*, "A global multi-hazard risk analysis of road and railway infrastructure assets," *Nature Communications*, vol. 10, no. 1, Art. no. 1, Jun. 2019, doi: 10.1038/s41467-019-10442-3.
- [9] C. Nicolas *et al.*, "Stronger Power: Improving Power Sector Resilience to Natural Hazards," World Bank, Washington, DC, Jun. 2019. doi: 10.1596/31910.
- [10] Thacker S. *et al.*, "Infrastructure for climate action," UNOPS, Copenhagen, Denmark., 2021. Accessed: Nov. 26, 2021. [Online]. Available: <https://www.unops.org/news-and-stories/news/infrastructure-for-climate-action>
- [11] "Sendai Framework for Disaster Risk Reduction 2015-2030," UNDRR, 2015. Accessed: Nov. 26, 2021. [Online]. Available: <https://www.undrr.org/publication/sendai-framework-disaster-risk-reduction-2015-2030>
- [12] "SWD(2013)318 - COMMISSION STAFF WORKING DOCUMENT on a new approach to the European Programme for Critical Infrastructure Protection Making European Critical Infrastructures more secure," European Commission, 2013. Accessed: Nov. 11, 2020. [Online]. Available: <https://ec.europa.eu/transparency/regdoc/?fuseaction=list&coteld=10102&year=2013&number=318&version=ALL&language=en>
- [13] S. M. Rinaldi, J. P. Peerenboom, and T. K. Kelly, "Identifying, understanding, and analyzing critical infrastructure interdependencies," *IEEE Control Systems Magazine*, vol. 21, no. 6, pp. 11–25, Dec. 2001, doi: 10.1109/37.969131.

- [14] D. Mitsova, A.-M. Esnard, A. Sapat, and B. S. Lai, "Socioeconomic vulnerability and electric power restoration timelines in Florida: the case of Hurricane Irma," *Nat Hazards*, vol. 94, no. 2, pp. 689–709, Nov. 2018, doi: 10.1007/s11069-018-3413-x.
- [15] ECA Working Group, "Shaping Climate-Resilient Development – A Framework for Decision-Making," 2009. Accessed: Jun. 05, 2020. [Online]. Available: https://ethz.ch/content/dam/ethz/special-interest/usys/ied/wcr-dam/documents/Economics_of_Climate_Adaptation_ECA.pdf
- [16] Stip, C., Z. Mao, G. Browder, L. Bonzanigo, and J. Tracy, "Water Infrastructure Resilience – Examples of Dams, Wastewater Treatment Plants, and Water Supply and Sanitation Systems," World Bank, Washington, DC, Sector note for LIFELINES: The Resilient Infrastructure Opportunity, 2019. [Online]. Available: <http://documents1.worldbank.org/curated/en/960111560794042138/pdf/Water-Infrastructure-Resilience-Examples-of-Dams-Wastewater-Treatment-Plants-and-Water-Supply-and-Sanitation-Systems.pdf>
- [17] S. Hallegatte, J. Rentschler, and J. Rozenberg, *Lifelines: The Resilient Infrastructure Opportunity*. World Bank Publications, 2019.
- [18] D. N. Bresch, J. Berghuijs, R. Egloff, and R. Kupers, "A Resilience Lens for Enterprise Risk Management," in *Turbulence: A Corporate Perspective on Collaborating for Resilience*, Amsterdam University Press, 2014, pp. 49–65. Accessed: Jun. 08, 2020. [Online]. Available: <https://www.research-collection.ethz.ch/handle/20.500.11850/127039>
- [19] R. J. Dawson *et al.*, "A systems framework for national assessment of climate risks to infrastructure," *Philosophical Transactions of the Royal Society A: Mathematical, Physical and Engineering Sciences*, vol. 376, no. 2121, p. 20170298, Jun. 2018, doi: 10.1098/rsta.2017.0298.
- [20] M. Ouyang, "Review on modeling and simulation of interdependent critical infrastructure systems," *Reliability Engineering & System Safety*, vol. 121, pp. 43–60, Jan. 2014, doi: 10.1016/j.res.2013.06.040.
- [21] E. E. Lee, J. E. Mitchell, and W. A. Wallace, "Network Flow Approaches for Analyzing and Managing Disruptions to Interdependent Infrastructure Systems," in *Wiley Handbook of Science and Technology for Homeland Security*, American Cancer Society, 2009, pp. 1–9. doi: 10.1002/9780470087923.hhs686.
- [22] R. A. Loggins and W. A. Wallace, "Rapid Assessment of Hurricane Damage and Disruption to Interdependent Civil Infrastructure Systems," *Journal of Infrastructure Systems*, vol. 21, no. 4, p. 04015005, Dec. 2015, doi: 10.1061/(ASCE)IS.1943-555X.0000249.
- [23] C. Zorn, R. Pant, S. Thacker, and A. Y. Shamseldin, "Evaluating the Magnitude and Spatial Extent of Disruptions Across Interdependent National Infrastructure Networks," *ASME J. Risk Uncertainty Part B*, vol. 6, no. 2, Jun. 2020, doi: 10.1115/1.4046327.
- [24] R. Pant, S. Thacker, J. W. Hall, D. Alderson, and S. Barr, "Critical infrastructure impact assessment due to flood exposure," *Journal of Flood Risk Management*, vol. 11, no. 1, pp. 22–33, 2018, doi: 10.1111/jfr3.12288.
- [25] R. Pant, J. W. Hall, and S. P. Blainey, "Vulnerability assessment framework for interdependent critical infrastructures: case-study for Great Britain's rail network," *European Journal of Transport and Infrastructure Research*, vol. 16, no. 1, Art. no. 1, Jan. 2016, doi: 10.18757/ejtir.2016.16.1.3120.
- [26] N. Goldbeck, P. Angeloudis, and W. Y. Ochieng, "Resilience assessment for interdependent urban infrastructure systems using dynamic network flow models," *Reliability Engineering & System Safety*, vol. 188, pp. 62–79, Aug. 2019, doi: 10.1016/j.res.2019.03.007.
- [27] C. Nan and G. Sansavini, "A quantitative method for assessing resilience of interdependent infrastructures," *Reliability Engineering & System Safety*, vol. 157, pp. 35–53, Jan. 2017, doi: 10.1016/j.res.2016.08.013.
- [28] L. Dueñas-Osorio, J. I. Craig, and B. J. Goodno, "Seismic response of critical interdependent networks," *Earthquake Engineering & Structural Dynamics*, vol. 36, no. 2, pp. 285–306, 2007, doi: 10.1002/eqe.626.
- [29] J. Banerjee, K. Basu, and A. Sen, "Analysing robustness in intra-dependent and inter-dependent networks using a new model of interdependency," *International Journal of Critical Infrastructures*, vol. 14, no. 2, pp. 156–181, Jan. 2018, doi: 10.1504/IJCIS.2018.091938.
- [30] M. Ouyang and L. Dueñas-Osorio, "An approach to design interface topologies across interdependent urban infrastructure systems," *Reliability Engineering & System Safety*, vol. 96, no. 11, pp. 1462–1473, Nov. 2011, doi: 10.1016/j.res.2011.06.002.
- [31] R. Guidotti, H. Chmielewski, V. Unnikrishnan, P. Gardoni, T. McAllister, and J. van de Lindt, "Modeling the resilience of critical infrastructure: the role of network dependencies," *Sustainable and Resilient Infrastructure*, vol. 1, no. 3–4, pp. 153–168, Nov. 2016, doi: 10.1080/23789689.2016.1254999.
- [32] S. Thacker, R. Pant, and J. W. Hall, "System-of-systems formulation and disruption analysis for multi-scale critical national infrastructures," *Reliability Engineering & System Safety*, vol. 167, pp. 30–41, Nov. 2017, doi: 10.1016/j.res.2017.04.023.
- [33] H. Masoomi, H. Burton, A. Tomar, and A. Mosleh, "Simulation-Based Assessment of Postearthquake Functionality of Buildings with Disruptions to Cross-Dependent Utility Networks," *Journal of Structural Engineering*, vol. 146, no. 5, p. 04020070, May 2020, doi: 10.1061/(ASCE)ST.1943-541X.0002555.
- [34] X. He and E. J. Cha, "Modeling the damage and recovery of interdependent civil infrastructure network using Dynamic Integrated Network model," *Sustainable and Resilient Infrastructure*, vol. 5, no. 3, pp. 152–167, May 2020, doi: 10.1080/23789689.2018.1448662.
- [35] I. Hernandez-Fajardo and L. Dueñas-Osorio, "Probabilistic study of cascading failures in complex interdependent lifeline systems," *Reliability Engineering & System Safety*, vol. 111, pp. 260–272, Mar. 2013, doi: 10.1016/j.res.2012.10.012.

- [36] D. Z. Tootaghaj, N. Bartolini, H. Khamfroush, T. He, N. R. Chaudhuri, and T. L. Porta, "Mitigation and Recovery From Cascading Failures in Interdependent Networks Under Uncertainty," *IEEE Transactions on Control of Network Systems*, vol. 6, no. 2, pp. 501–514, Jun. 2019, doi: 10.1109/TCNS.2018.2843168.
- [37] H. Fotouhi, S. Moryadee, and E. Miller-Hooks, "Quantifying the resilience of an urban traffic-electric power coupled system," *Reliability Engineering & System Safety*, vol. 163, pp. 79–94, Jul. 2017, doi: 10.1016/j.res.2017.01.026.
- [38] J. Beyza, H. F. Ruiz-Paredes, E. Garcia-Paricio, and J. M. Yusta, "Assessing the criticality of interdependent power and gas systems using complex networks and load flow techniques," *Physica A: Statistical Mechanics and its Applications*, vol. 540, p. 123169, Feb. 2020, doi: 10.1016/j.physa.2019.123169.
- [39] M. Garschagen and S. Sandholz, "The role of minimum supply and social vulnerability assessment for governing critical infrastructure failure: current gaps and future agenda," *Natural Hazards and Earth System Sciences*, vol. 18, no. 4, pp. 1233–1246, Apr. 2018, doi: <https://doi.org/10.5194/nhess-18-1233-2018>.
- [40] S. E. Chang, T. L. McDaniels, J. Mikawoz, and K. Peterson, "Infrastructure failure interdependencies in extreme events: power outage consequences in the 1998 Ice Storm," *Nat Hazards*, vol. 41, no. 2, pp. 337–358, May 2007, doi: 10.1007/s11069-006-9039-4.
- [41] D. B. Karakoc, K. Barker, C. W. Zobel, and Y. Almoghathawi, "Social vulnerability and equity perspectives on interdependent infrastructure network component importance," *Sustainable Cities and Society*, vol. 57, p. 102072, Jun. 2020, doi: 10.1016/j.scs.2020.102072.
- [42] S. E. Chang, C. Pasion, S. Yavari, and K. Elwood, "Social Impacts of Lifeline Losses: Modeling Displaced Populations and Health Care Functionality," pp. 1–10, Apr. 2012, doi: 10.1061/41050(357)54.
- [43] R. Pant, J. W. Hall, and S. Thacker, "System-of-systems framework for global infrastructure vulnerability assessments," 2017. Accessed: Nov. 03, 2020. [Online]. Available: <https://www.greengrowthknowledge.org/sites/default/files/downloads/resource/System-of-systems%20framework%20for%20global%20infrastructure%20vulnerability%20assessments.pdf>
- [44] E. Zio, "Challenges in the vulnerability and risk analysis of critical infrastructures," *Reliability Engineering & System Safety*, vol. 152, pp. 137–150, Aug. 2016, doi: 10.1016/j.res.2016.02.009.
- [45] G. Aznar-Siguan and D. N. Bresch, "CLIMADA v1: a global weather and climate risk assessment platform," *Geoscientific Model Development*, vol. 12, no. 7, pp. 3085–3097, Jul. 2019, doi: 10.5194/gmd-12-3085-2019.
- [46] WorldPop, "Global 1km Population total adjusted to match the corresponding UNPD estimate." University of Southampton, Jun. 22, 2020. doi: 10.5258/SOTON/WP00671.
- [47] P. Gauthier, A. Furno, and N.-E. El Faouzi, "Road Network Resilience: How to Identify Critical Links Subject to Day-to-Day Disruptions," *Transportation Research Record*, vol. 2672, no. 1, pp. 54–65, Dec. 2018, doi: 10.1177/0361198118792115.
- [48] H. Chmielewski, R. Guidotti, T. McAllister, and P. Gardoni, "Response of Water Systems under Extreme Events: A Comprehensive Approach to Modeling Water System Resilience," pp. 475–486, May 2016, doi: 10.1061/9780784479865.050.
- [49] M. Ouyang, L. Hong, Z.-J. Mao, M.-H. Yu, and F. Qi, "A methodological approach to analyze vulnerability of interdependent infrastructures," *Simulation Modelling Practice and Theory*, vol. 17, no. 5, pp. 817–828, May 2009, doi: 10.1016/j.simpat.2009.02.001.
- [50] D. N. Bresch and G. Aznar-Siguan, "CLIMADA v1.4.1: towards a globally consistent adaptation options appraisal tool," *Geoscientific Model Development*, vol. 14, no. 1, pp. 351–363, Jan. 2021, doi: 10.5194/gmd-14-351-2021.
- [51] S. Eberenz, S. Lüthi, and D. N. Bresch, "Regional tropical cyclone impact functions for globally consistent risk assessments," *Natural Hazards and Earth System Sciences*, vol. 21, no. 1, pp. 393–415, Jan. 2021, doi: <https://doi.org/10.5194/nhess-21-393-2021>.
- [52] I. J. Sauer *et al.*, "Climate signals in river flood damages emerge under sound regional disaggregation," *Nature Communications*, vol. 12, no. 1, Art. no. 1, Apr. 2021, doi: 10.1038/s41467-021-22153-9.
- [53] P. M. Kam *et al.*, "Global warming and population change both heighten future risk of human displacement due to river floods," *Environ. Res. Lett.*, vol. 16, no. 4, p. 044026, Mar. 2021, doi: 10.1088/1748-9326/abd26c.
- [54] M. Souvignet, F. Wieneke, L. Mueller, and D. N. Bresch, "Economics of Climate Adaptation (ECA) - Guidebook for Practitioners," 2016.
- [55] "Managing the Risks of Extreme Events and Disasters to Advance Climate Change Adaptation," IPCC, 2012. Accessed: Aug. 17, 2022. [Online]. Available: <https://www.ipcc.ch/report/managing-the-risks-of-extreme-events-and-disasters-to-advance-climate-change-adaptation/>
- [56] S. Eberenz, D. Stocker, T. Rössli, and D. N. Bresch, "Asset exposure data for global physical risk assessment," *Earth System Science Data*, vol. 12, no. 2, pp. 817–833, Apr. 2020, doi: 10.3929/ethz-b-000409595.
- [57] S. Eberenz, S. Lüthi, and D. N. Bresch, "Regional tropical cyclone impact functions for globally consistent risk assessments," *Natural Hazards and Earth System Sciences*, vol. 21, no. 1, pp. 393–415, Jan. 2021, doi: <https://doi.org/10.5194/nhess-21-393-2021>.
- [58] F. Pianosi *et al.*, "Sensitivity analysis of environmental models: A systematic review with practical workflow," *Environmental Modelling & Software*, vol. 79, pp. 214–232, May 2016, doi: 10.1016/j.envsoft.2016.02.008.
- [59] A. Tabandeh, N. Sharma, and P. Gardoni, "Uncertainty propagation in risk and resilience analysis of hierarchical systems," *Reliability Engineering & System Safety*, vol. 219, p. 108208, Mar. 2022, doi: 10.1016/j.res.2021.108208.

- [60] C. M. Kropf *et al.*, "Uncertainty and sensitivity analysis for probabilistic weather and climate risk modelling: an implementation in CLIMADA v.3.1.," Feb. 2022, Accessed: Mar. 18, 2022. [Online]. Available: <https://eartharxiv.org/repository/view/3123/>
- [61] N. Bloemendaal, H. de Moel, J. M. Mol, P. R. M. Bosma, A. N. Polen, and J. M. Collins, "Adequately reflecting the severity of tropical cyclones using the new Tropical Cyclone Severity Scale," *Environ. Res. Lett.*, vol. 16, no. 1, p. 014048, Jan. 2021, doi: 10.1088/1748-9326/abd131.
- [62] K. R. Knapp, M. C. Kruk, D. H. Levinson, H. J. Diamond, and C. J. Neumann, "The International Best Track Archive for Climate Stewardship (IBTrACS): Unifying Tropical Cyclone Data," *Bulletin of the American Meteorological Society*, vol. 91, no. 3, pp. 363–376, Mar. 2010, doi: 10.1175/2009BAMS2755.1.
- [63] G. Holland, "A Revised Hurricane Pressure–Wind Model," *Mon. Wea. Rev.*, vol. 136, no. 9, pp. 3432–3445, Sep. 2008, doi: 10.1175/2008MWR2395.1.
- [64] R. Fausset, A. Blinder, and M. Haag, "Rescue Teams Scour Ruins as Hurricane Death Toll Rises," *The New York Times*, Oct. 12, 2018. Accessed: Feb. 14, 2022. [Online]. Available: <https://www.nytimes.com/2018/10/12/us/hurricane-michael-live-updates-florida.html>
- [65] E. Jenelius and L.-G. Mattsson, "Road network vulnerability analysis of area-covering disruptions: A grid-based approach with case study," *Transportation Research Part A: Policy and Practice*, vol. 46, no. 5, pp. 746–760, Jun. 2012, doi: 10.1016/j.tra.2012.02.003.
- [66] K. M. de Bruijn, L. Cumiskey, R. N. Dhubhda, M. Hounjet, and W. Hynes, "Flood vulnerability of critical infrastructure in Cork, Ireland," *E3S Web Conf.*, vol. 7, p. 07005, 2016, doi: 10.1051/e3sconf/20160707005.
- [67] L. Iannacone, N. Sharma, A. Tabandeh, and P. Gardoni, "Modeling Time-varying Reliability and Resilience of Deteriorating Infrastructure," *Reliability Engineering & System Safety*, vol. 217, p. 108074, Jan. 2022, doi: 10.1016/j.ress.2021.108074.
- [68] H. Holma, P. Kinnunen, I. Z. Kovács, K. Pajukoski, K. Pedersen, and J. Reunanen, "Performance," in *LTE for UMTS*, John Wiley & Sons, Ltd, 2011, pp. 257–301. doi: 10.1002/9781119992943.ch10.
- [69] De Leonardis, D., Huey, R., and Green, J., "National Traffic Speeds Survey III: 2015," National Highway Traffic Safety Administration, Washington, DC, DOT HS 812 485, Mar. 2018.
- [70] P. Gauthier, A. Furno, and N.-E. El Faouzi, "Road Network Resilience: How to Identify Critical Links Subject to Day-to-Day Disruptions," *Transportation Research Record*, vol. 2672, no. 1, pp. 54–65, Dec. 2018, doi: 10.1177/0361198118792115.
- [71] C. R. Zorn and A. Y. Shamseldin, "Quantifying Directional Dependencies from Infrastructure Restoration Data," *Earthquake Spectra*, vol. 32, no. 3, pp. 1363–1381, Aug. 2016, doi: 10.1193/013015EQS015M.
- [72] C. Zorn, R. Pant, S. Thacker, and A. Y. Shamseldin, "Evaluating the Magnitude and Spatial Extent of Disruptions Across Interdependent National Infrastructure Networks," *ASME J. Risk Uncertainty Part B*, vol. 6, no. 2, Jun. 2020, doi: 10.1115/1.4046327.
- [73] E. Luijijf, A. Nieuwenhuijs, M. Klaver, M. van Eeten, and E. Cruz, "Empirical Findings on Critical Infrastructure Dependencies in Europe," in *Critical Information Infrastructure Security*, Berlin, Heidelberg, 2009, pp. 302–310. doi: 10.1007/978-3-642-03552-4_28.
- [74] N. Sharma and P. Gardoni, "Mathematical modeling of interdependent infrastructure: An object-oriented approach for generalized network-system analysis," *Reliability Engineering & System Safety*, vol. 217, p. 108042, Jan. 2022, doi: 10.1016/j.ress.2021.108042.
- [75] K. Poljansek, M. Marín Ferrer, T. De Groeve, and I. Clark, "Science for disaster risk management 2017: knowing better and losing less," ETH Zurich, Report, 2017. Accessed: Jun. 08, 2020. [Online]. Available: <https://www.research-collection.ethz.ch/handle/20.500.11850/297819>
- [76] A. Naqvi and I. Monasterolo, "Natural Disasters, Cascading Losses, and Economic Complexity: A Multi-layer Behavioral Network Approach," Apr. 2019. <https://epub.wu.ac.at/6914/> (accessed Apr. 28, 2022).
- [77] A. Otsuka, "Natural disasters and electricity consumption behavior: a case study of the 2011 Great East Japan Earthquake," *Asia-Pac J Reg Sci*, vol. 3, no. 3, pp. 887–910, Oct. 2019, doi: 10.1007/s41685-019-00129-4.
- [78] M. Ghosn *et al.*, "Performance Indicators for Structural Systems and Infrastructure Networks," *Journal of Structural Engineering*, vol. 142, no. 9, p. F4016003, Sep. 2016, doi: 10.1061/(ASCE)ST.1943-541X.0001542.
- [79] D. Henry and J. Emmanuel Ramirez-Marquez, "Generic metrics and quantitative approaches for system resilience as a function of time," *Reliability Engineering & System Safety*, vol. 99, pp. 114–122, Mar. 2012, doi: 10.1016/j.ress.2011.09.002.
- [80] Y. Almoghathawi, K. Barker, and L. A. Albert, "Resilience-driven restoration model for interdependent infrastructure networks," *Reliability Engineering & System Safety*, vol. 185, pp. 12–23, May 2019, doi: 10.1016/j.ress.2018.12.006.
- [81] L. I. E. E., J. E. Mitchell, and W. A. Wallace, "Restoration of Services in Interdependent Infrastructure Systems: A Network Flows Approach," *IEEE Transactions on Systems, Man, and Cybernetics, Part C (Applications and Reviews)*, vol. 37, no. 6, pp. 1303–1317, Nov. 2007, doi: 10.1109/TSMCC.2007.905859.
- [82] S. Hasan and G. Foliente, "Modeling infrastructure system interdependencies and socioeconomic impacts of failure in extreme events: emerging R&D challenges," *Nat Hazards*, vol. 78, no. 3, pp. 2143–2168, Sep. 2015, doi: 10.1007/s11069-015-1814-7.
- [83] D. Mitsova, A. Sapat, A.-M. Esnard, and A. J. Lamadrid, "Evaluating the Impact of Infrastructure Interdependencies on the Emergency Services Sector and Critical Support Functions Using an Expert Opinion Survey," *Journal of Infrastructure Systems*, vol. 26, no. 2, p. 04020015, Jun. 2020, doi: 10.1061/(ASCE)IS.1943-555X.0000548.

- [84] S. L. Cutter, B. J. Boruff, and W. L. Shirley, "Social Vulnerability to Environmental Hazards," in *Hazards Vulnerability and Environmental Justice*, Routledge, 2006.
- [85] G. Holland, "A Revised Hurricane Pressure–Wind Model," *Mon. Wea. Rev.*, vol. 136, no. 9, pp. 3432–3445, Sep. 2008, doi: 10.1175/2008MWR2395.1.
- [86] J. Guo, T. Feng, Z. Cai, X. Lian, and W. Tang, "Vulnerability Assessment for Power Transmission Lines under Typhoon Weather Based on a Cascading Failure State Transition Diagram," *Energies*, vol. 13, no. 14, 2020, doi: <http://dx.doi.org/10.3390/en13143681>.
- [87] "Hazardus Hurricane Model Technical Manual," FEMA, Mar. 2021. Accessed: Mar. 10, 2022. [Online]. Available: https://www.fema.gov/sites/default/files/documents/fema_hazus-hurricane-technical-manual-4.2.3_0.pdf

Annex

A. Formal treatment of the developed modelling chain

G^j	graph of CI network j
n_i^j	i^{th} node in G^j
e_{mn}^j	directed edge from n_m^j to n_n^j
G	interdependent CI graph, spanning all graphs G^j, G^k, \dots of investigated CI networks and all e^{jk}
e_{mn}^{jk}	directed dependency edge from n_m^j to n_n^k
$G^{j'}$	subgraph of G spanning all elements of G^j
$G^{j'jk}$	subgraph of G , spanning all elements G^j, G^k and e^{jk}
A^{jk}	adjacency matrix of $G^{j'jk}$
L_i	geo-spatial location of graph element i (node and edge attribute)
F_i	functional state of graph element i (node and edge attribute)
I_i	structural damage ('impact') of graph element i (node and edge attribute)
E_i	exposure value of graph element i (node and edge attribute)
D_i	damage threshold of graph element i (node and edge attribute)
C_i^{jk}	capacity for node i for type of flow passing between CI types j and k (node attribute)
T_i^{jk}	capacity threshold for node i for type of flow passing between CI types j and k (node attribute)
M_i^{jk}	capacity supply at node i for type of flow passing between CI types j and k (node attribute)
S_i^j	service supply at node i for type of flow delivered by CI type j (node attribute)
$H(L)$	hazard intensity at geographic location L
$V(H)$	hazard intensity-dependent vulnerability curve

Initialization

0. $\forall j$ create G^j with n^j (nodes-only) or n^j, e^j (nodes and edges) and set attributes L, F, D, E, X

L : geo-location in latitude and longitude; specific to each n_i^j, e_i^j

F : functional state $\{0, 1\}$. Set to 1 $\forall n^j, e^j \in G^j$

D : fraction $[0, 1]$ of structural damage I beyond which $F \rightarrow 0$; specific to n^j, e^j

E : value of the physical network element - set to 1 $\forall n^j, e^j \in G^j$

X : further attributes specific to n^j and/or e^j

1. Create interdependent CI graph $G = \sum_j G^j$

\forall combinations of (jk) in list of identified CI dependencies:

Create e_{mn}^{jk} between n_m^j and n_n^k if linking conditions (distance, redundancy criterion, etc.) fulfilled

Assign node attributes $C^{jk}, T^{jk} \forall n \in G$:

$$C_i^{jk} : \begin{cases} -1 & \text{if } n_i^j \\ 1 & \text{if } n_i^k \\ 0 & \text{else} \end{cases}, T_i^{jk} : \begin{cases} [0, 1] & n_i^k \\ 0 & \text{else} \end{cases}$$

Flow Assignment & Functional State Update

2. $\forall j$ where $G^j \ni n^j, e^j$: extract $G^{j'}$ from G .

Perform internal flow calculations according to adequate algorithm.

Update $C^{jk}, F \forall n^j$ in G , where required.

3. \forall combinations of (jk) where $k \neq \text{'people'}$, extract $G^{j'jk}$ from G ; update $F \forall n^k$:

$$M^{jk} = (F \cdot C^{jk})^T * A^{jk}; F = \min(F, M^{jk} \geq T^{jk})$$

4. Repeat 2. and 3. until $\Delta F = 0$

Basic Service Access Determination

5. \forall combinations of (j, people) , extract $G^{j, \text{people}}$ from G . Assign attribute S^j to n^{people} :

$$M^{j, \text{people}} = (F \cdot C^{j, \text{people}})^T * A^{j, \text{people}}$$

$$S^j = (M^{j, \text{people}} \geq T^{j, \text{people}})$$

Natural Hazard Impact Calculation & Functionality State Update

6. Assign structural damage attribute $I \forall n, e \in G$:

$$I = H(L) * V(H) * E$$

7. Update $F \forall n, e \in G$:

$$F = \min(F, I \leq D)$$

Cascade & Functionality State Updates

8. Update $C^{jk}, F \forall n, e \forall (jk, k \neq \text{people})$ in G according to 2. - 4.

Basic Service Access Update

9. If road access is a linking condition for dependency combination (j, people) :

Re-check path existence and length of path between $n^j, n^{\text{people}} \forall e^{j, \text{people}}$; else delete $e^{j, \text{people}}$ from G

10. Update $S^j \forall n^{\text{people}}, \forall (j, \text{people})$; see step 5.

B. Modelling Choices for CI Networks

Table B.1 CI networks and their components, in edges (E) and nodes (N). First column suggests a simple sub-selection of network components to represent the systems in a standardized low-complexity setting, second column proposes additional components if data is available.

CI system	Simplified representation	Extension possibilities
Road	N: intersections E: streets	N: tunnels, bridges E: -
Electric Power	N: power generation plants E: transmission lines	N: transmission & distribution substations, power poles E: low-voltage distribution lines
Telecommunication	N: cell towers E: -	N: internet exchange points, data centres, central offices, base stations, poles E: landlines, fibre-optic cables, submarine transmission lines
Wastewater & Water Supply	N: water treatment plants E: -	N: wells, reservoirs, tanks, cisterns, pumps, water bodies E: water pipelines, water tunnels, rivers
Healthcare & Emergency Services	N: hospitals, clinics E: -	N: doctors' practices, dentists, pharmacies, nursing homes
Educational Facilities	N: schools E:	N: universities, childcare centres, kindergartens
End-users	N: people clusters E: -	

C. Case Study

C.1. Infrastructure System Model Inputs

C.1.1 Infrastructure Component Data

Table C.1 Geo-coded infrastructure asset data used in the case study, section 3. *) HIFLD: Homeland Infrastructure Foundation-Level Data

Infrastructure	Source	Data description, Pre-processing
Roads	OpenStreetMap	<i>Data:</i> Retrieved from data dump at geofabrik.de for states FL, AL, GA matching tags highway= (motorway motorway_link trunk trunk_link primary primary_link) using the OpenStreetMap module in CLIMADA. <i>Pre-processing:</i> Line merging, roundabout cleaning, duplicate removal, linking unconnected cluster
Hospitals	HIFLD*: Hospitals	<i>Data:</i> All amenities in states FL, AL, GA incl. 20kms buffer around outer borders <i>Pre-processing:</i> -
Power lines	HIFLD: Electric Power Transmission Lines	<i>Data:</i> All lines in in states FL, AL, G <i>Pre-processing:</i> Line merging, duplicate removal, linking unconnected cluster
Power plants	HIFLD: Power Plants	<i>Data:</i> All amenities in states FL, AL, GA incl. 20 km buffer around outer borders <i>Pre-processing:</i> -
Educational facilities	HIFLD: Public Schools	<i>Data:</i> All amenities in states FL, AL, GA incl. 20 km buffer around outer borders <i>Pre-processing:</i> -
Cell towers	HIFLD: Cellular Towers	<i>Data:</i> All amenities in states FL, AL, GA incl. 20 km buffer around outer borders <i>Pre-processing:</i> -
Wastewater	HIFLD: Wastewater Treatment Plants	<i>Data:</i> All amenities in states FL, AL, GA incl. 20 km buffer around outer borders <i>Pre-processing:</i> -
People	WorldPop Gridded Population Count	<i>Data:</i> United States of America, 1km UN-adjusted, 2020. <i>Pre-processing:</i> Re-gridded raster data on population counts to resolution of 10 km x10 km, vectorized, cropped at outer borders of states FL, AL, GA

C.1.2 Power Supply & Demand Data

Table C.2 Population data, energy supply and demand data used for case study in section 3.

Variable	Source	Data description
Supply	HIFLD: Power Plants	Same data source as for geo-location data of power plants in the region of interest. Electric energy supply taken from power plants net annual generation, given in column <i>NET_GEN</i> .
Demand	International Energy Agency (IEA) World Energy Balances	Total electric energy consumption for entire USA, all sectors, 2019.

Calculation of electric power demand per people cluster (cf. Table C.1): Total electric energy consumption / total US-population * population count of cluster

Calculation of electric power supply per power plant (cf. Table C.1): Directly taken from data source.

Supply / demand balancing in undisrupted state: Addition of an import/export element to the power plant data frame with supply amounting to difference between total power plants supply in region of interest and total energy consumption in region of interest.

C.1.3 Dependencies

Table C.3 Dependencies identified between CI networks (#1-#6) and between CI networks and end-users (#7-#12). Dependency parametrizations are used to link individual CI graphs and population graph into one interdependent CI graph. Decisions for certain parameter settings are discussed in the paragraph below.

Dep	Source	Target	Redundancy	Road access	Dep. type	Flow type	Func. Thresh	Dist. Thresh. [m]
1	power line	celltower	TRUE	FALSE	functional	physical	0.6	
2	power line	education	TRUE	FALSE	functional	physical	0.6	
3	wastewater	education	TRUE	FALSE	functional	logical	1	
4	power line	health	TRUE	FALSE	functional	physical	0.6	
5	wastewater	health	TRUE	FALSE	functional	logical	1	
6	power line	wastewater	TRUE	FALSE	functional	physical	0.6	
7	celltower	people	FALSE	FALSE	end user	logical	1	30000
8	education	people	TRUE	TRUE	end user	logical	1	40000
9	health	people	FALSE	TRUE	end user	logical	1	100000
10	power line	people	TRUE	FALSE	end user	physical	0.6	
11	road	people	FALSE	FALSE	end user	logical	1	30000
12	wastewater	people	TRUE	FALSE	end user	logical	1	

Selection of distance thresholds: A combination of sophisticated guess (such as 30 km being a generous diameter for cell tower reach [68] or hospitals being at most 100 km from persons, which equals a travel time of little more than the “golden hour” crucial in medical emergencies, when considering average travel speeds on a highway [69]), and iterative refinements such that service access levels in stage IV were >99% for all basic services across the area of investigation in a base state simulation with undamaged CIs. For instance, setting cell tower ranges to 15 km would have resulted in 6.7 M customers without mobile communication access in the base state, whereas the hence chosen range (30 km) resulted in only a few hundred persons without coverage. For dependencies where no distance thresholds are set, target elements are linked to the closest element of the respective source type, irrespective of its distance. This is the case for all non-redundant dependencies where it is obvious that such a link must exist (e.g. educational and healthcare facilities having power and water access).

Selection of redundancy specification: Water and power are modelled to be supplied through a single source per dependent target. Mobile communication is modelled to be provided from any source within distance thresholds, as connectivity can be established through any reachable cell site. Healthcare can be provided from any reachable healthcare facility, but school enrolments are usually fixed, hence each population clusters dispose of only one non-substitutable education link. Road access is assumed to be provided by any reachable road within the given distance threshold.

Selection of flow types and functionality thresholds: Physical variables for power demand and supply across the modelled area were available and capacity in the network is hence calculated as the ratio of power demand to power supply in each network cluster. Functionality thresholds for power dependencies could therefore be expressed as a continuous fraction

with regard to the capacity ratio. It was set here to 0.6 in absence of any component-specific information, to interpreted as “if demand-to-supply ratio in the power network cluster to which the dependent component is linked, drops below 0.6, the component will turn dysfunctional”. All other dependencies are, in absence of physically informed flow metrics, logical dependencies. As such, they either provide supply from a functional source, or they do not, if the source is dysfunctional. Functionality thresholds for logical dependencies are hence trivial and set to 1. Road paths between population nodes and social facilities (hospitals, schools) were computed based on a Dijkstra’s shortest path algorithm.

C.1.4 Infrastructure Interdependent CI Graph Specifications

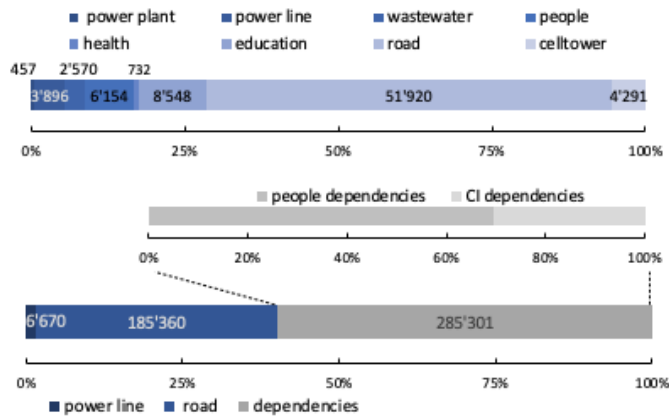


Figure C.1 Specifications of node (1st bar plot) and edge elements (2nd bar plot) in the interdependent CI graph, constructed for the case presented in section 3.1.

C.2. Natural Hazard Risk Model Inputs

C.2.1 Hazard Footprint

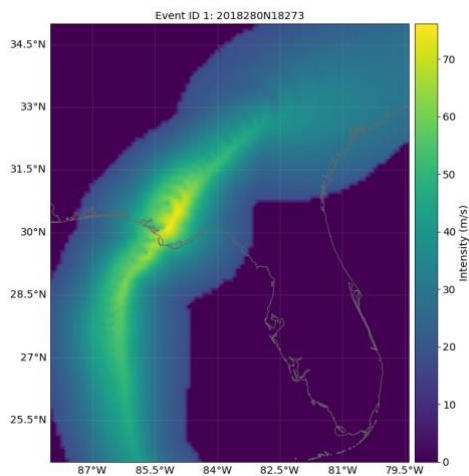


Figure C.2 Map of Hurricane Michael wind-field intensity, computed with CLIMADA from Michael’s hurricane track. Track data from IBTrACS, implemented wind field algorithm from [85].

C.2.2 Vulnerability Curves

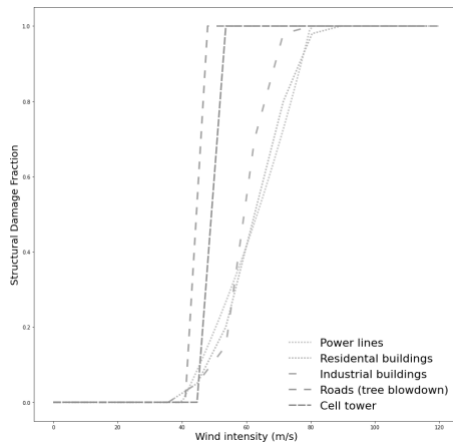


Figure C.3 Impact functions used for structural damage calculations from hurricane wind field in section 3.1, for all CI types. Note that y-axis represents fraction of structural damage to components for all CIs except power lines, for which it is failure probability. Sources: power lines in [58], residential building and industrial building (both for $z=0.35$) in [87], roads in [8], cell towers: step function taken from interview with cell tower provider stating they are “built to withstand winds of up to 110 miles per hour”.

C.3. Scenario Analysis

C.3.1 Scenario Selection and Results Overview

Table C.4 Scenarios to study the sensitivity of end results (number of people experiencing basic service disruptions) to assumptions throughout the modelling chain. For parameterizations details, see supplementary material.

Scenario	Description	Stage
No CI inter-dependencies	Removing any functional dependencies between CI networks.	I
Longer path threshold	Increasing allowed distance thresholds for end-user travel paths	I / IV
Shorter path threshold	Decreasing allowed distance thresholds for end-user travel paths	I / IV
Low component vulnerability	Shifting impact functions to withstand higher hazard intensities.	II
High component vulnerability	Shifting impact functions to withstand lower hazard intensities.	II
Low functionality threshold	Decreasing damage thresholds for component dysfunctionality.	II
High functionality threshold	Increasing damage thresholds for component dysfunctionality.	II

Table C.5 Results of scenario analysis: Amount of people experiencing service disruptions in each scenario due to hazard-induced failure cascades, relative to disruption numbers in the originally chosen parametrization as described in section 3.1. The 7 selected scenarios are described in Table C.4 and discussed in section 0. Parametrizations of the scenarios are listed in the supplementary material.

Access to Basic Service	original	No CI Inter-dep.	Longer path thresh.	Shorter path thresh.	Low vulnerability	High vulnerability	Low funct. thresh.	High funct. thresh.
Mobility	100	100	100	100	205	42	116	81
Power	100	88	95	90	238	37	96	66
Healthcare	100	48	97	142	196	48	115	80
Education	100	72	100	121	236	45	106	87
Mobile Comms.	100	57	95	96	236	30	92	61
Water Supply	100	45	100	103	232	24	100	100

C.3.2 Scenario Parametrizations

See Supplementary Material.

C.4. Validation Sources

See Supplementary Material.